DESIGN AND MANAGEMENT OF DC MICROGRID SYSTEM

2023
MASTER THESIS
ELECTRICAL AND ELECTRONICS ENGINEERING

Waleed Khalid Abdulkareem AL-BAYATI

Thesis Advisor
Assist. Prof. Dr. Selçuk A. AVCI

DESIGN AND MANAGEMENT OF DC MICROGRID SYSTEM

Waleed Khalid Abdulkareem AL-BAYATI

Thesis Advisor

Assist. Prof. Dr. Selçuk A. AVCI

T.C.

Karabük University

Institute of Graduate Programs

Department of Electrical and Electronics Engineering

Prepared as

Master Thesis

KARABUK

January 2023

I certify that in my opinion the thesis submitted by Waleed Khalid Abdulkareem AL-BAYATI titled “DESIGN AND MANAGEMENT OF DC MICROGRID SYSTEM” is fully adequate in scope and quality as a thesis for the degree of Master of Science.

Assist. Prof. Dr. Selçuk A. AVCI .....
Thesis Advisor, Department of Electrical and Electronics Engineering

This thesis is accepted by the examining committee with a unanimous vote in the Department of Electrical and Electronics Engineering as a Master of Science thesis. 20/01/2023

Examining Committee Members (Institutions)	Signature
Chairman : Prof. Dr. Ziyodulla YUSUPOV (KBÜ)	.....
Member : Assist. Prof. Dr. Selçuk A. AVCI (KBÜ)	.....
Member : Assist. Prof. Dr. Cevat RAHEBI (İTOÜ)	.....

The degree of by the thesis submitted is approved by the Administrative Board of the Institute of Graduate Programs, Karabuk University.

Prof. Dr. Müslüm KUZU .....
Director of the Institute of Graduate Programs

“I declare that all the information within this thesis has been gathered and presented in accordance with academic regulations and ethical principles and I have according to the requirements of these regulations and principles cited all those which do not originate in this work as well.”

Waleed Khalid Abdulkareem AL-BAYATI

ABSTRACT

M. Sc. Thesis

DESIGN AND MANAGEMENT OF DC MICROGRID SYSTEM

Waleed Khalid Abdulkareem AL-BAYATI

Karabük University
Institute of Graduate Programs
The Department of Electrical and Electronics Engineering

Thesis Advisor:
Assist. Prof. Dr. Selçuk A. AVCI
January 2023, 71 pages

Solar energy sources can supply power during day only and with specific ratings depends on the PV array capacity and the irradiance level, therefore it must be utilized as maximum as possible. But in sometimes the produced peak power is more than the load demand, and that leads to store the remained energy either in the grid by using grid connected inverters or by using a storage device such as battery storage system. In this work a grid connected DC microgrid with storage system and PV array with 10 kW capacity is simulated. A P&O maximum power point tracking algorithm will be used so as to tracking the maximum power point (MPP) for the PV array system. The studied DC microgrid contains AC and DC loads. The proposed system is simulated for all expected operating cases. The simulation is done using MATLAB/Simulink program. The simulation's findings demonstrate that the PV array always suplies the most power in all studied scenarios. Load sharing depends on the produced power from the PV array and the stored energy in the battery system. The priority is to supply the

load with the necessary electrical energy from the PV array and then the batteries, and if there is more demand the utility grid will supply it.

Key Words : Solar Energy, Microgrids, Mppt, P&O, Peak Power.
Science Code : 90513

ÖZET

Yüksek Lisans Tezi

DC MİKROGRİD SİMÜLASYONU VE YÖNETİMİ

Waleed Khalid Abdulkareem AL-BAYATI

Karabük Üniversitesi
Lisansüstü Eğitim Enstitüsü
Elektrik ve Elektronik Mühendisliği Anabilim Dalı

Tez Danışmanı:
Assist. Prof. Dr. Selçuk A. AVCI
Ocak 2023, 71 sayfa

Güneş enerjisi kaynakları yalnızca gün boyunca güç sağlayabilir ve PV dizi kapasitesine ve ışınım düzeyine bağlı olarak belirli derecelendirmelerle güç sağlayabilir, bu nedenle mümkün olduğu kadar maksimum düzeyde kullanılmalıdır. Ancak bazen üretilen tepe gücü, yük talebinden daha fazladır ve bu, kalan enerjinin şebekeye bağlı invertörler kullanılarak veya pil depolama sistemi gibi bir depolama cihazı kullanılarak şebekede depolanmasına yol açar. Bu çalışmada, depolama sistemli şebeke bağlantılı bir DC mikro şebekesi ve 10 kW kapasiteli PV dizisi simüle edilmiştir. PV dizisi için maksimum güç noktasını izlemek için bir P&O maksimum güç noktası izleme algoritması kullanılır. İncelenen DC mikro şebekesi, AC ve DC yükleri içerir. Önerilen sistem, tüm beklenen çalışma durumları için simüle edilmiştir. MATLAB/Simulink programı kullanılarak simülasyon yapılmıştır. Simülasyon sonuçları, simüle edilen tüm durumlarda PV dizisinin maksimum gücü sağladığını ve yük paylaşımının PV dizisinden üretilen güce ve akü sisteminde depolanan enerjiye bağlı olduğunu göstermektedir. Öncelik, yüke gerekli elektrik enerjisini PV dizisinden

ve ardından pillerden sağlamaktır ve daha fazla talep varsa, elektrik şebekesi bunu sağlayacaktır.

Anahtar Kelimeler : Güneş Enerjisi, Mikro Şebekeler, Mppt, P&O, Tepe Güç.
Bilim Kodu : 90513

ACKNOWLEDGMENT

I would like to acknowledge and give my warmest thanks to my supervisor (Assist. Prof. Dr. Selcuk A. AVCI) who made this work possible. His guidance and advice carried me through all the stages of writing my project. I would also like to thank my committee members for letting my defense be an enjoyable moment, and for your brilliant comments and suggestions, thanks to you.

I would also like to express my special thanks to my family as a whole for their continuous support and understanding when undertaking my research and writing my project. Your prayers for me was what sustained me this far.

Finally, I would like to thank Allah, for letting me through all the difficulties. You are the one who let me finish my degree. I will keep on trusting you for my future.

CONTENTS

Page

Page

Page

LIST OF FIGURES

Page

Page

Page

LIST OF TABLES

Page

SYMBOLS AND ABBREVIATIONS

SYMBOLS

W	: Watt
V	: Volt
A	: Ampere
Hz	: Hertz
Ipv	: PV array current
Id	: Diode current
Ish	: Short circuit current
q	: Electron charge
K	: The Boltzmann’s constant
T	: Temperature
N	: Number of cells
Rs	: Series resistance
Rsh	: Shunt resistance
Iph	: Photon current
ΔV	: Voltage change
Δp	: Power change
dP	: Power derivative
dV	: Voltage derivative
Vin	: Input voltage
Vout	: Output voltage
D	: Duty cycle

ABBREVIATIONS

DER	: Distributed energy resources
IEEE	: The Institute of Electrical and Electronics Engineers

CERTS : The Consortium for Electric Reliability Technology Solutions

Std. : Standard

AC : Alternative current

DC : Direct current

ESS : Energy storage system

PV : Photovoltaic

LVDC : Low voltage direct current

EMS : Energy management system

MPPT : Maximum power point tracking

PWM : Pulse width modulation

DGs : Distributed generators

CHP : Combined heat power

PCS : Power control system

ZVS : Zero voltage switching

SC : Supper capacitor

SCESS : Supper capacitor energy management system

BESS : Battery energy management system

MPC : Model predictive system

GA : Genetic algorithm

TOU : Time of use

GCH : Grid connected home

NPC : Neutral point clamping

SOC : State of charge

VSI : Voltage source inverter

PLL : Phase locked loop

P&O : Perturb and observe

IGBT : Isolated gate bipolar transistor

PART 1

INTRODUCTION

1.1. BACKGROUND

The power system is designed to be developed into a smart grid that is safer, greener, and more efficient [1][2]. This progressive transition can help to achieve the environmental objectives, embodies grid-end user interactions, and promotes large-scale combination of distributed energy resources (DER). Microgrids need progressive management methods in addition to power control techniques.

The distributed energy resources (DERs) systems, that convert electricity from high level voltage systems to medium and low-level voltage costumers, are essential nexuses that feed power flows in the power system [3]. DERs such as renewable resources, energy storage system, and distributed power generators [4] are commonly medium to low level voltage power devices and normally transfer power through distributed systems. With a speedily increasing numbers of DERs, distributed systems are meeting unfamiliar challenges in addition to opportunities. Let's say, by the year of 2030, DERs will observe for approximately 30% of the universal gross power electricity generation [5], accordingly a friendlier environmentally electricity power system can be constructed with optimized energy efficiency and reduced impurity emissions. Nevertheless, the increased growing of DERs' penetration could lead to a bigger danger of generation-expending imbalance as a result of the intermittent nature of several DERs. Consequently, stability associated problems may occur: deteriorated power quality, oscillatory frequency, and unbalanced voltage are basically immediate aftermath of a load destabilizing. Many protocols, such as IEEE Std. 1547 [6], were launched in practice that establish high standards for operation of the distributed systems embedded with DERs. Unfortunately, outdated distributed systems, that were designed many years ago only to provide basic local loads, can hardly operate to

encounter these strict desires. More progressive form of association of the DERs is compulsory to significantly enable their integration.

A microgrid system, which locally matches DERs with different local loads, is an emergent form of distributed power system [7]. Microgrids will constitute a significant building block for future smart grids in that they have a two-fold advantage: initially, in case of emergency it can withdraw from the faulted traditional main grid, and organizes resident DERs to deliver reliable power supply for the local loads; secondly, when it's associated with the traditional main grid, it also utilizes as a one of friendly manageable power asset to provide main-grid with power. Represented microgrid system project [8] demonstrates that the use of microgrid systems implement requirements like IEEE Std. 1547 and optimizes the dynamic performance of DERs [9].

There are two common categories of microgrid systems, namely direct current (DC) and alternating current (AC) microgrids. Fig. 1.1 shows a typical DC microgrid. In terms of several considerations DC microgrids can be more advantageous than the AC counterpart once DC components are predominant.

Actually, various power components nowadays are in DC, ranging from renewable energy resources (RES) such as photovoltaic (PV), to energy storage systems (ESS) such as battery packs, and to different loads such as various plug-in electric vehicles. On one hand, DC microgrids basically have higher efficiency of power transmission by shrinking stages of DC/AC power conversions.

As stated by [10], a significant enhancement of no less than 4% - 6% in efficiency could be estimated from DC systems if compared to well-designed AC systems currently. On the other hand, DC microgrids have a way concise but effective control objectives. Dissimilar its AC counterpart, DC microgrids have only active power flow therefore maintaining only the level of voltage stability guarantees the critical generations load balance. Due to these benefits, DC microgrids are finding in more applications such as electric airplanes, modern data centers, and ships as well.

1.2. PROBLEM STATEMENTS

Various types of loads are exponentially increasing in today's technologically advanced society, necessitating the construction of power production systems and transmission amenities every year. Nevertheless, a new, potential paradigm is emerging from two angles as a universal energy challenge. The initial step is to promote and expand alternative energy sources that rely on green and renewable energy sources (RESs), such wind and solar power. Another step is to research DC microgrids, which can increase the performance effectiveness of power distribution by lowering the number of energy conversion steps and by developing an entirely new, superior efficiency energy tool to match up with the growing demand for numerous digital loads. Due to this, researches, articles, and studies on DC microgrid systems and distributed energy resources (DERs) that use clean and renewable energy are quickly increasing worldwide.

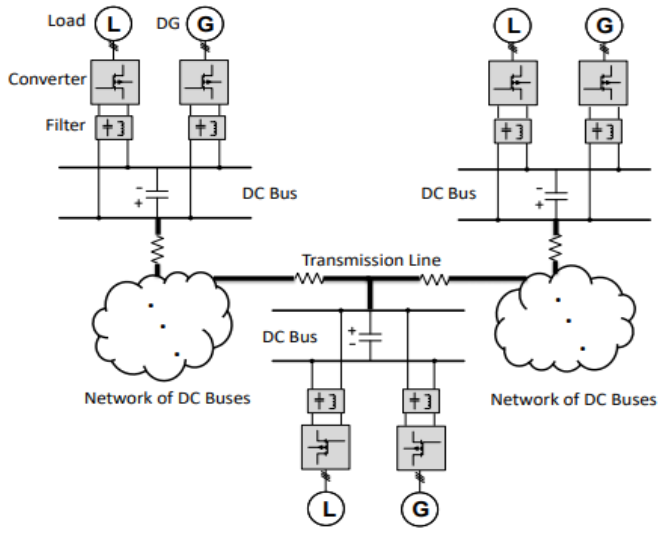

Figure 1.1. Typical DC microgrid system.

DC Low voltage direct current (LVDC) microgrids are mostly utilized for distributed electronic devices used in daily living, such like office-based electronic equipment, light emitting diodes (LED), and battery charging stations, which their voltage value ranges from 150 Vdc to 1500 Vdc. [11][12]. Numerous distributed energy resources (DERs) are used in such a DC microgrid, and these resources are associated with renewable energy sources (RESs), which have recently received attention as

distributed generating systems (DGs). In this instance, intermittent power generation occurs because there is ambiguity over the supplied power value in the DC microgrid [13]. Additionally, since significant variations in the DC microgrid's voltage and power value are to be expected, the load type in the system is also instantaneously variable. To resolve this, an energy management system (EMS) is needed to implement smart and stable operation for the DC microgrid's energy storage system (ESS).

1.3. THESIS OBJECTIVES

This thesis aims to design and management of a DC microgrid that dynamically enhance the operation of DC microgrids, which comprising of a battery branch, photovoltaic (PV), and DC bus, to consistently regulate DC bus voltage level, manage power flows from source to load and perform charging \ discharging processes of batteries in the microgrid system.

The suggested strategy is a maximum power point tracker (MPPT) that hire renewable power systems as flexible generators which means that the produced power of renewable energy systems is optimally reduced, if required, in proportion to their ratings.

1.4. METHODOLOGY OF THE RESEARCH

A small island's microgrid is modeled and developed using direct current (DC) with a connection to the main grid. Photovoltaic power cells are used as a main power generating resources to produce power and provide it to the loads. The design and simulation of the different microgrid system components are achieved using MATLAB/Simulink. Maximum power point trackers (MPPT) and photovoltaic (PV) modules are combined with power electronic converters to manage the DC bus voltage and to get the most out of the solar resource. One operation modes will be used in this system which is MPP operation mood. A bidirectional converter (BDC) is similarly proposed to manage power flowing from energy storage system (ESS) to connected loads or the opposite. A PI controller is used to control the buck-boost bidirectional converter so as to achieve the energy managing process. Energy storage system (ESS)

comprised of lead-acid battery and Bi-directional converter is used to supply a smooth output power to the load when there are fluctuations with the generated power by the photovoltaic system. The system simulation flowchart is shown in figure 1.2.

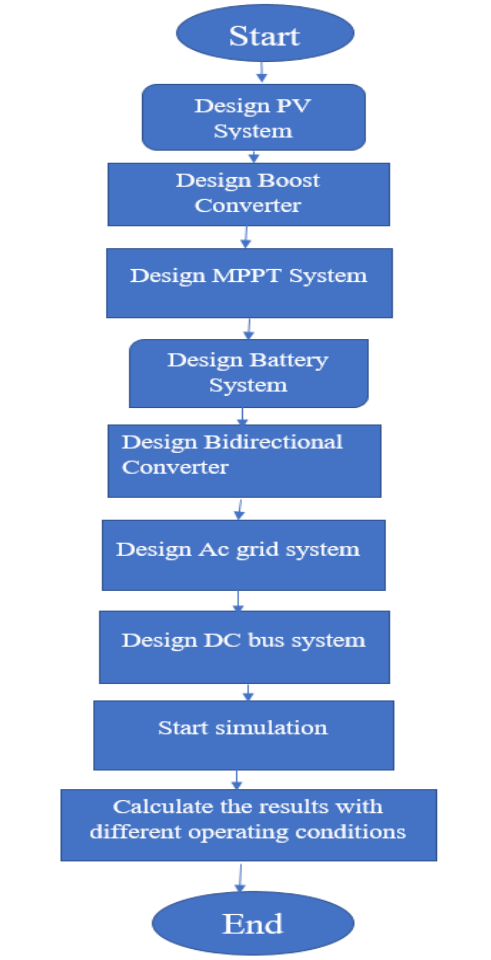

Figure 1.2. Methodology flowchart.

1.5. THESIS OUTLINES

CHAPTER ONE represents general background of microgrids, problem statement, thesis objectives, thesis methodology and thesis outlines.

CHAPTER TWO represents basic concepts of DC microgrids in addition to literature review of the thesis.

CHAPTER THREE represents photovoltaic cell theory in addition to maximum power point tacking concept.

CHAPTER FOUR represents the simulation of Circuit diagram and results.

CHAPTER FIFE represents conclusion of thesis and recommended future work.

PART 2

LITERATURE REVIEW

2.1. MICROGRIDS

Microgrid is a modern system that includes the collecting of different distributed generating resources (DGs), power bank system and loads can help the traditional power grid in some areas where the distributed generation is available by providing reliable, sustainable, and price-competitive costs power to the users. Power or energy flow one-way from huge synchronous generator machines through a transmitting or distribution network to the end-users in the extremely centralized traditional power systems. However, the environmental challenges brought on by the burning of fossil fuels and the technological issues with conventional electric services have necessitated the need to develop a new power system technology.

The advancement of distributed energy resource (DER) systems such as wind, photovoltaic (PV), biomass, battery, micro-turbine, fuel cell, etc. has generated interest in these technologies. An efficient method of integrating such DER units into power grid systems is the use of microgrid systems. Actually, we don't have as a specific definition of the microgrid and the definition can vary according to different regions or countries. Figure 2.1 shows a typical structure of a microgrid, containing DGs, such as PV systems, wind power systems, combined heat and power unit (CHP), micro-turbines, fuel cells; a distributed energy storage (DES) systems like batteries, super-capacitors, electric vehicles flywheels; various flexible loads and control elements. We can classify microgrids as AC, DC & hybrid types.

Although AC microgrids can be interconnected to the traditional AC grid, complex control procedures are necessary throughout the synchronization process to maintain the stability of the system. Unlikely, DC microgrids have improved efficiency and

better short circuit protection. Within the same microgrid system, we typically link certain non-synchronous elements (like as micro-turbine machines) in addition to some synchronous elements (like as diesel generators). The capacity of extra DC loads, particularly Plug-in Hybrid Electric Vehicles, may be increased, making the dual AC/DC synchronous and non-synchronous microgrid system types through multiple (two-ways) route converters progressively more desirable. Figure 2.2 illustrates the typical network topology of a hybrid AC/DC microgrid, which includes power electronic connections and several DER units. [13].

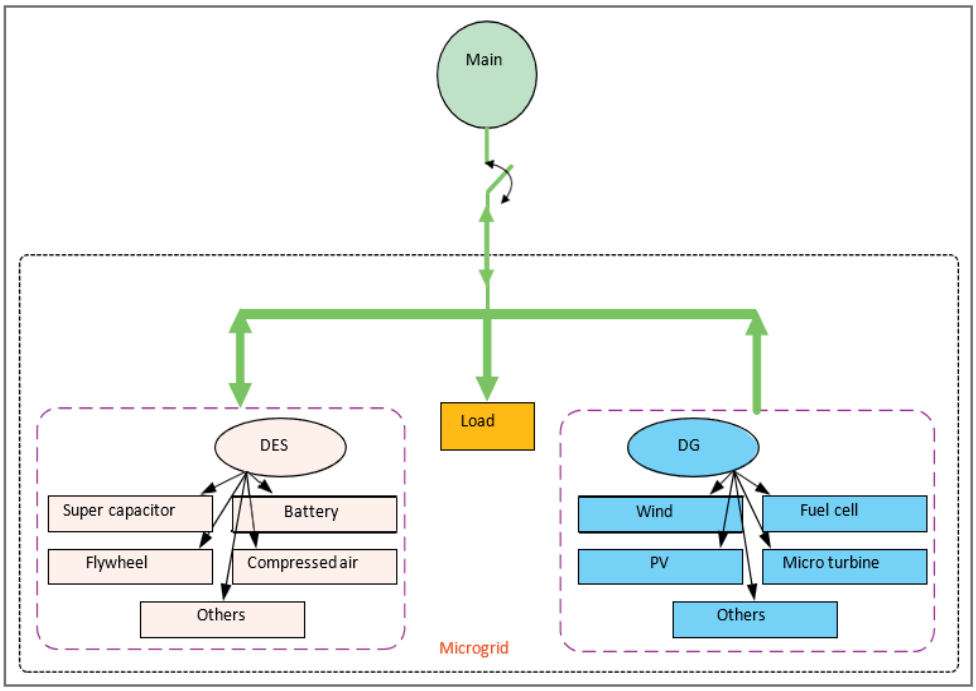

Figure 2.1. Typical structure of a microgrid.

2.1.1. DC Microgrids

Microgrids can be AC, DC or hybrid type. Each type of them has advantages and disadvantages. Due to DC microgrids, we can see that the power electronic interfaces are simple which lead to fewer points of failure. Also, imbalances issues are not available in this system as well as no harmonic, no reactive power, and high efficiency over the traditional AC grid [14].

In spite of these advantages, we can see some challenges face the system such as; the adoption as unanimity system, relevant problems to the power system protection, lack of people who are experienced with the system and lack of standard transmission lines that are used in the system. All of these challenges represent obstacles face the dc microgrids [14].

2.1.2. Distributed Energy Resources (DERs)

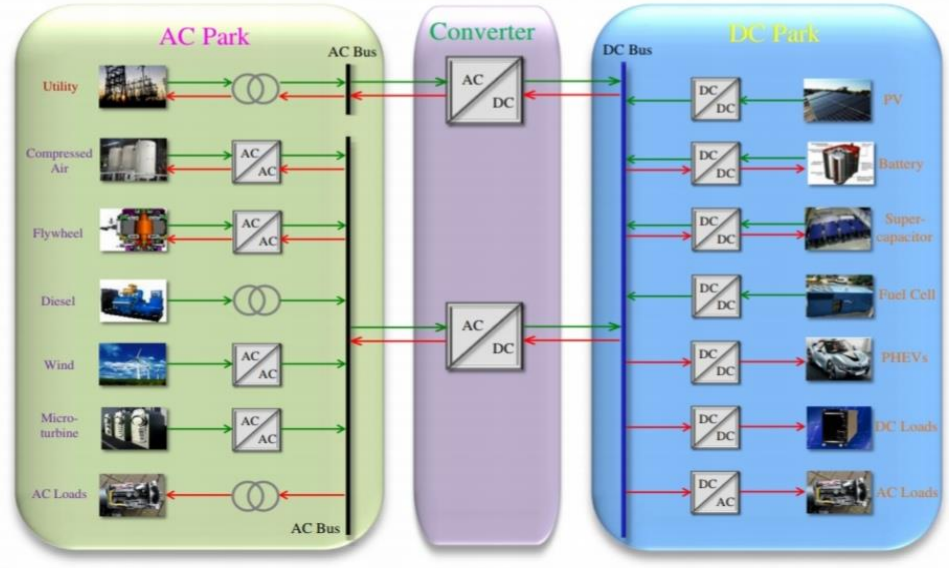

Figure 2.2. Hybrid microgrid typical system structure

Distributed energy resources can be defined as different types of technologies that provide electricity and placed near to the end-users. The electrical power system was created in a distributed formation but for economical consecrations in production and transmission consecrations the system has been developed to a large scale and an interconnected one. The DERs involve several types such as photovoltaic (PV), turbine generator, combined heat and power (CHP), engine generator, microturbine, fuel cell, wind power, energy storage, hydro generator. The DERs' nearness to the end-users in the microgrids can bring numerous advantages to both the costumer and the utilities, such providing high power quality, reducing energy transmission losses, increasing consistency during upstream fault situations, [15][16]. Figure 2.3 shows distributed .Energy Resources Register.

Figure 2.3. Distributed energy resources register

2.1.3. Renewable and Non-renewable Resources

Due to the type of power used to generate the electricity, we can classify The DERs into two groups: non-renewable energy resources and renewable energy resources. The first group: non-renewable energy resources similar the traditional generators, which produce electricity from fossil fuels such as natural gas, coal and petroleum [17].

In the other hand, the second group: renewable energy resources generate electricity from unreliable sources such as wind, sunlight, geothermal heat and tides, etc., [18]. Lately, we got started noticing that the growing up of renewable energy resources in microgrids is significant and quite rapid due to the several factors such as world-wide energy policy, the concern of greenhouse gas emission and global warming. However, despite of these advantages, they have a disadvantage that the generated power is not permanent over time. It is because the amount of generated power from the renewable energy resources depends directly to the weather conditions such as decreasing solar irradiance decreases the amount of generated power. And this drawback of renewable energy resources makes it unreliable in microgrids [19].

2.2. GRID CONNECTED DC MICROGRIDS

DC microgrid systems are able to run either independently in grid-connected mode by connecting to the utility grid at a point of shared coupling through an inverter or in islanded mode [20]. As illustrated in Figure 2.4, a DC microgrid consists of a PV system, AC loads, and a connected inverter that transmits the remaining energy in grid-connected mode to the main grid after supplying power to the load. The DC microgrid control system must provide optimal current sharing across converters based on their ratings while also reducing voltage variation [21].

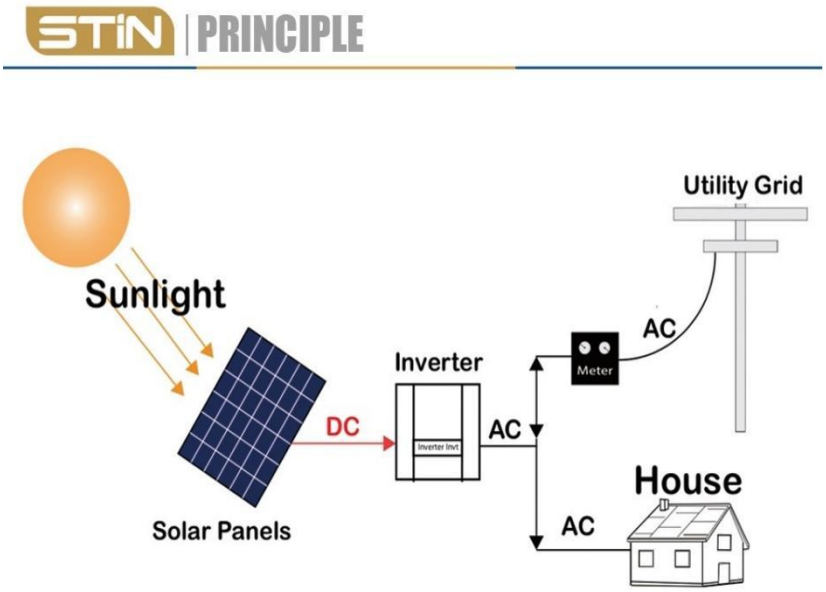

Figure 2.4. Grid connected DC microgrid system.

Many approaches, like as master-slave and droop control, are utilized to control DC microgrids. In the master-slave control technique, the master converter is in charge of controlling the voltage level of the DC microgrid system and sending signals to the other converters so that the load may be powered. This method is less reliable since the breakdown of the master converter immediately will lead to the breakdown of the entire system. [22]. The droop control approach is extensively utilized when all converters are in charge of managing the voltage of a DC microgrid system. In the droop control method, both of parameters: droop resistance and reference voltage should be specified for each converter. In the second approach, the droop resistance value can be calculated by using the converter rating. Even though the droop approach

is considered as an efficient method, it includes several downsides, like lesser precision of current sharing among multiple converters owing to the effects of the line resistance linking each converter to the microgrid, and the microgrid's voltage decreases with loading [23].

2.3. ENERGY CONTROLLING CONCEPT

Solving power management issues was the main task of a number of investigators during the past decades, through conducting a lot of activities and experiments. Energy management means controlling the flowing power from the source to the load. And in order to achieve this purpose; many different power control techniques are developed. Power control techniques in the microgrid principally goals to achieve the following targets;

1. Ability and flexibility to add or remove new distributed generation systems (DGs) and distributed storage system (DS) in the microgrids without any causing impact to the system
2. Ability to regulate the variation in the common DC bus voltage easily and flexibly
3. Ensure proper energy flow controlling and balancing within the microgrid
4. Enable stable sharing of current between parallel power converters, and the essential goal of power management circuit is to fulfill power balance.

Microgrid power flow controlling targets to economic power transmitting [24]. The power flow management can be categorized into two approaches: optimization-based and rule-based. In the first method, managing the power of system is done through mathematical optimization, and executed with constraints and objective function. But a rule-based method runs the power of system with respect to prefixed rules, like simple rules, identified by a multi-agent system and based on fuzzy logic methods. The optimization process should take into account the forecast of different renewable energy generation and load power demand while satisfying many constraints [24].

2.4. LITERATURE REVIEW

Energy management of DC microgrid can be considered one of the most important challenges faces distributed generation systems due to their intermittent nature in power producing of these systems. Therefore, enhancing control power flowing system will assist to increasing the reliability for such systems by providing customers with permanent power. that's why too many researchers dealt with it in their researches.

In [25], the researcher presented a model of parallel-series two-bridge DC/DC converter topology able to work beside ZVS over a wide value of input and load. Researcher achieved in his application a power managing system (PCS) of photovoltaic (PV) panels that used as a power generator in hybrid renewable energy system. A scheme with two units of freedom that was developed by the researcher allows the PV-PCS to regulate the DC-link voltage while the PV panel tracks its maximum power point (MPP). Researcher concluded that the used converter is capable of regulating the DC-coupling bus voltage in addition to performing the maximum power tacking process perfectly to extract the maximum from the PV panel simultaneously.

In [26], the reader published a search titled by "Energy Management Strategy for Supercapacitor in Droop-controlled DC Microgrid Using Virtual Impedance" studied on it the ability of integrating super-capacitor (SC) into a droop-controlled DC microgrid as an autonomous super-capacitor energy storage system (SCESS). Researcher proposed a novel power flow control strategy for SCESS. He used a virtual impedance loop to apply the virtual resistor in addition to a virtual capacitor which is linked in series between the DC-coupling bus and the used converter that confirms the plug and play feature while separating the power flowing between SCESS and other DGs. The results of the search showed that the suggested energy management system includes a competing dynamic performance associated with exceptional flexibility as compared to other existing methods.

In [27], the researchers: Anu Varghese, Lekshmi R. Chandran and Arun Rajendran addressed a coordinated power flow management strategy within DC microgrid for proper energy managing between power generating units and customers in addition to regulation of DC-coupling bus voltage. Researchers developed a separated control scheme for battery charging and discharging. Researchers concluded that the used control method could balance the power between different distributed power resources and customers in a DC microgrid in case of extreme condition. Furthermore, they ensured that working of low-voltage DC microgrid can be validate under different operating cases.

In [28], the publisher developed and implemented a new prototype model of the power flow controlling system of a DC microgrid in islanded mode comprising of battery with ultra-capacitor creating Hybrid Energy Storage System (HESS) in order to extending battery lifecycle. Researchers implemented the microgrid with power electronic dc-dc converters controlled using close loop control and they achieved the control method using fuzzy logic scheme carried out in microcontroller. Researchers tested the system under variable load environments and concluded that appropriate working of the system comprising of PV cells panel and hybrid energy storage system can be ensured. In furthermore, using ultra-capacitor would build op lifecycle of battery and provide more amount of energy over a short period of time.

In [29], the auditor studied various modeling techniques in order to demonstrating scalability in addition to modularity of DC microgrid systems. Researcher developed a flexible state-space modeling technique in order to perfectly representing a complete DC microgrid system to explore the power generation sources that have on stability and effects of additional energy storage mean. Researcher proposed an autonomous power management scheme in order to furthering DC microgrid reliability and robustness. Researcher concluded that DC microgrids systems have the probable to be a scalable, modular solution that can be integrated with renewable power sources and basic BESS technology. The sizeable energy scaling abilities and quick-response autonomous power management methods reveal the potential to evolve a robust distributed grid substructure.

Also in [30], the researcher developed control schemes for DC-bus voltage regulation and maximum power point tracking (MPPT) of islanded DC-microgrids. The DC microgrid in case of consideration comprises of PV array system, constant power loads, battery and fixed resistance loads. Researcher derived a dynamic model for the DC microgrid system and he designated it by a multi-output and multi-input nonlinear system with non-affine inputs. Relied on the non-linear dynamic model that already has built researcher employs the output regulation concept in order to designing a local-state feedback control law which controls the DC-bus voltages to propose set points and maximizes the extracted output power from the PV.

Researcher proposed three different control strategies, constant feedback, measurement feedback and state feedback. Researcher validated the efficiency of the proposed control schemes by simulations while occurring both of illumination and load changing.

In [31] authors assume when it comes to creating a long-term power supply system, RES is gaining traction in Japan, where the private sector has integrated a large number of distributed photovoltaic systems into the public grid. Author's primary focus in this research is to examine the long-term technical and economic performance of residential PV systems in Kyushu, Japan, with and without battery systems, with a nominal capacity of 5.0 KWP. Instead of focusing just on the aggregated impacts of grid-tied home PV batteries, we additionally investigate the aggregated effects of optimum dispatch of power flows in demand. A bottom-up method to peak balancing is used to optimize the battery to maximize PV self-consumption and help relieve the load on the battery. Following extensive testing in Kyushu-style homes using the proposed residential PV battery concept, the following findings may be summarized:

1. As battery size grows, the self-consumption ratio of PV cells rises non-linearly until it reaches a saturation point.
2. While monthly self-consumption rates might vary greatly from month to month, self-consumption rates tend to be higher during the winter season because of the comparatively low PV generation capabilities.

3. Assuming a 2 percent share of the total grid load, an aggregated residential PV battery system (assuming 1.1 percent of net peak load) can contribute to releasing peak pressure against the need for grid flexibility.

In [32], the publishers proposed a method of power flow controlling strategy relied on a Model Predictive Control (MPC) technique for photovoltaic (PV) cells /battery storage system in an islanded DC microgrid. Researchers considered that PV-Battery system is presented using a non-linear model with four operating modes. Moreover, they formulated an optimization problem encounter the voltage performance in the system according to operating modes and constraints. Researchers concluded that the used controller guarantees to provide required power to the customers by discharging battery storage in case of lacking of generated power from PV system or emergency variations in load demands.

Again in [33], the reader proposed a design and simulation for a DC microgrid system in a small island called belize. The system included renewable energy production resources. Researcher selected a cost affordable system in order to encountering the load necessities of the small island and the financial profits of the DC microgrid system have been calculated over an AC microgrid. Researcher conducted financial analysis using the model of Hybrid Optimization for Electric Renewables (HOMER) software. Researcher from carried out simulations concluded that voltage can be stabilized and the bi-directional converter was functioned correctly. Moreover, he estimated that the microgrid can cover15.7% Island from PV arrays and 10 containers for storage batteries. As a result, he proposed to size up both of diesel generators to meeting sudden peak load with hydrogen storage and solar generators to meeting the normal load.

In [34], the publisher showed that the residential photovoltaic (PV) generating systems linked to the grid have seen significant growth in China in the last several years. In a house PV power system, three various sorts of power sources—PV generation, battery bank, and the main grid be properly arranged. People in China have come to accept the usage of the time of use tax and the step tariff. Two optimum energy management techniques for home power systems are thus proposed in this research in order to

accommodate the two tariffs and achieve maximum advantages. Optimizing the home energy costs is the goal of these solutions, and the transmitting ratio of power supplied to the grid and consumed locally serves as an optimization variable. So, Method of Genetic algorithms (GA) are used to tackle the nonlinear optimization problems posed. Verification is done on a typical household power system that includes grid-connected PV arrays and a battery bank system. A GA-based solution approach, coupled with the suggested energy management methods, is successful in planning the operation status of the three power resources to maximize economic advantages under the time-of-use tariff and step tariff, respectively, according to the findings of the study.

In [35], the publisher explained that in order to meet the rising need for energy while also addressing environmental concerns, individuals have begun exploring and implementing new and more environmentally friendly energy sources. For an unstable grid-tied solar power system in Larkana, Pakistan, this paper provides an ideal system setup for dependable power production. In order to meet the goal, the research makes use of HOMER Pro simulation software and the necessary inputs. The financial side of the suggested system keep in mind the effects of planned and unplanned power outages, temperature, and the tilte angle of PV modules. Residential, deferred, and all peak loads are considered to be 13.2 kWh/day, 0.52 kWh/day, and 0.6 kW, respectively, in this study. Compared to an unstable grid/PV system, unreliable network power system with battery bank has a COE that is 48% more expensive. Compared to a stand-alone reliable grid without battery bank, the suggested system is determined to be more economically and ecologically viable.

In [36], the researcher has used the flat and time-of-use (TOU) electricity rate choices, this research conducts a comparison analysis to determine the practical optimum size of rooftop solar photovoltaic (PV) and Energy storage systems (ESSs) for grid-connected homes (GCHs). PV-BESS and PV-only systems were scaled to minimize the net percentage cost of power for four variations of electricity tariffs. Consideration of grid limits, daily supply of charge of power, solar and battery deterioration, real load and solar data, and the current market pricing of components were used to create a viable model. A rule-based energy management system for GCHs was developed in order to regulate the flow of power throughout PV, ESS, load, and grid. Grid

constraints and power tariffs, as well as component sizes, are the subjects of a number of sensitivity assessments. Accordingly, this article uses a grid-connected home in Australia to illustrate the capacity optimization model's applicability to any given situation. For the PV-BESS setup, the TOU-Flat option had the lowest NPC of all of the configurations or alternatives tested. According to two performance metrics, the ideal rooftop PV and BESS capacities are 9 kW and 6 kWh for the PV-BESS system with TOU-Flat: cost of energy in the present and future.

In [37], the auditor introduced a model of decentralized power management strategy for DC microgrids that operate in islanded mode in order to ensuring long-term operating heath besides protection for the used battery energy storage systems. He was ensuring that DC microgrids are totally effective for mixing solar photovoltaic cells as power producers with energy storage system (ESS) and variable local loads because of their simplicity of power conversion using converters and control schemes. The model utilized variable-intercept droop characteristic modifications in order to balancing the state-of-charge for multiple storage system elements in addition to a renewable source limiter in order to avoiding overcharging for batteries. He concluded that the decentralized nature for the modeled energy management system facilitates accommodating multiple power sources and storage devises into DC microgrids in the basis of plug-and-play. Researcher also discovered that the test setup of laboratory scale DC microgrid can be completed with programmable control devises and monitoring systems.

In [38], the reader determined that behind-the-meter photovoltaic (PV) paired with lithium-ion battery bank for commercial buildings might be economically viable utilizing HOMER Grid software, with a flat rate and TOU rate. According to the result of this research, the battery deterioration limit has been described as having an impact on the system's cost-effectiveness, as well as proving the influence of tariff rates on commercial buildings with variable energy use over a 25-year period. According to our findings, the system owner may save a significant amount of money by postponing the replacement of the battery storage. Since the battery will only need to be replaced once instead of twice, letting the battery to decline 50 percent of its original capacity results in a 30 percent decrease in the battery capital fee throughout the course of the

project. The degradation limit and tariff structure have an impact on a building's capacity to profit from solar-plus-storage, but the load pattern and size have little impact. We've come to the conclusion that by lowering their cost, TOU tariffs will hasten the deployment of PV systems with batteries in commercial projects.

In [39], the readers proposed an energy management system (EMS) that permits it to be utilized in both of stand-alone mode and grid - connected mode with 10 modes. With the purpose to obtain each mode in EMS, researcher considered in addition to the quantity of generated power, state of charge (SOC) of the battery bank and load power, furthermore the amount of rated power for the power storage system converter that implements charging and discharging processes. Researcher fabricated a laboratory-scale DC microgrid to conducting experimental authentication for the suggested EMS. Researcher concluded several points: firstly, ability of combining individual power conversion elements and availability of control approaches for integrated operation DC microgrids. Secondly, ability of simply implementing for the operation method of proposed EMS as comparing with conventional complicated research. Thirdly, ability of fabricating the laboratory scale of DC microgrid verifying the suggested EMS in actual experiment conditions. Lastly, ability of implementing of the suggested EMS for both of stand-alone mode and grid-connected that made installing of DC microgrids in real applications is more practical and feasible.

In [40], Jamshaid Mannan and others during 2021 have developed an innovative technique for utilizing photovoltaic (PV) energy system. First, a linear model technique is used to outline the issue, and then a cost function is created to assess the tariff under various conditions. In a restricted context, the goal of the cost function is to reduce the burden on customers. Intelligent utilization of battery storage devices lowers the costs of imported and exported energy. As long as the main battery system's charge level falls below a certain threshold, the secondary battery system drains. A wide range of tariff incentives are taken into account as part of the study. The study looks at the stand-alone PV systems, grid supply, PV systems associated with the traditional grid, and PV systems connected to the grid with energy storage banks. Based on unmet and surplus power, the statistical analysis is done in each scenario to provide a thorough look at ensuing distributed import/export/storage energy

distributions. According to the findings, the suggested solution saves £ 46 in imported and exported electricity costs.

In [41], the researchers explained that as renewable energy sources become more prevalent and solar irradiation fluctuates, energy storage is essential for addressing a variety of stability challenges in the power grid. According to [40], grid-connected home photovoltaic systems with hybrid power storage comprising of battery and super capacitor are designed and stabilized. In a fully active parallel design, two buck-boost bidirectional DC-DC converters couple the battery and supercapacitor containers to the shared 400 V DC-bus system. So their voltage quantities vary and their power flow is independently managed. The current controllers for the supercapacitor, battery and bidirectional converters are designed with small-signal stability in mind. The battery and supercapacitor converters' boost and buck modes of operation were thoroughly analyzed, resulting in more precise controller tuning. This is a crucial contribution. When developing the DC-bus voltage controller, which employs a phase-locked loop (PLL) for grid synchronization, the voltage source inverter's (VSI) small-signal stability analysis is also taken into consideration. The suggested model is based on mathematical analysis and average modeling and is created and simulated in the MATLAB/Simulink software environment. The results of the simulation show that the suggested model is dynamic, as shown by multiple quick shifts in PV production and load demand. There is a very minimal ripple voltage on the DC-bus and the model operates correctly and quickly throughout various mode changes (a maximum of 0.625 percent). As a final benefit, since the super-capacitor is capable of dealing with the fast changes that occur in under two seconds, it reduces the load on the battery and extends its lifespan.

2.5. SCOPE OF CHAPTER

In this section, researcher included the main sections for this part. In section 2.1, researcher presented a general introduction of microgrids then he pointed to distributed energy resources (DERs) including renewable\ non- renewable power generation resources and lastly, he explained the grid connected type of DC microgrids. In section 2.2, researcher presented grid connected DC microgrids. In 2.3,

researcher presented energy management concepts and he showed the power management techniques with their feedbacks. In section 2.4, the researcher characterized the literature reviews of DC microgrids which represent the backbone of the thesis, researcher presented and cited by 16 previous researches done on the related topic and he briefly demonstrated the results and goals were achieved for each research. In section 2.5, researcher presented the scope of the chapter which demonstrate the main sections of the chapter.

PART 3

DC-MICRO GRID SYSTEM MODELLING

3.1. INTRODUCTION

The proposed system represents a DC microgrid system, with a PV array system as a renewable energy source, storage device with charging controller and a DC common bus. The microgrid system has coupled to the main utility grid by the use of uncontrolled full bridge rectifier. Each part of the proposed system explained in detail in this chapter. Figure 3.1 shows the overall system Simulink model.

3.2. SOLAR PV SYSTEM MODELLING

Since each photovoltaic panel is composed of a sequence of linked solar cells, solar cells are the smallest components of a photovoltaic system. The solar cell generates electricity using the heat and light from solar radiation [42]. The amount of sunshine hitting the solar cell at any one time directly correlates to the energy production of the cell. Understanding how a solar panel may be improved, we must first comprehend a solar cell's electrical properties.

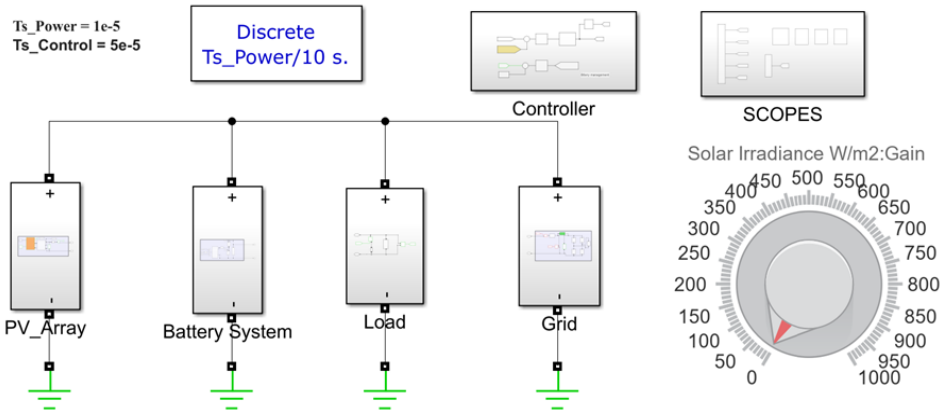

Figure 3.1. Simulink model for the proposed system.

The single diode model of this equivalent photovoltaic cell has been identified. The circuit in figure 3.2 can simulate the behavior of a PV cell, which is a non-linear source. The model enables complete mathematical characterization of the solar cell activity. The model's objective is to determine how temperature, solar radiation, voltage, current, and maximum power generation are related. Following that, a voltage-current characteristic may be shown. In order to plot the characteristic curve for the PV panel, the next section shows how to approximatively calculate the required values.

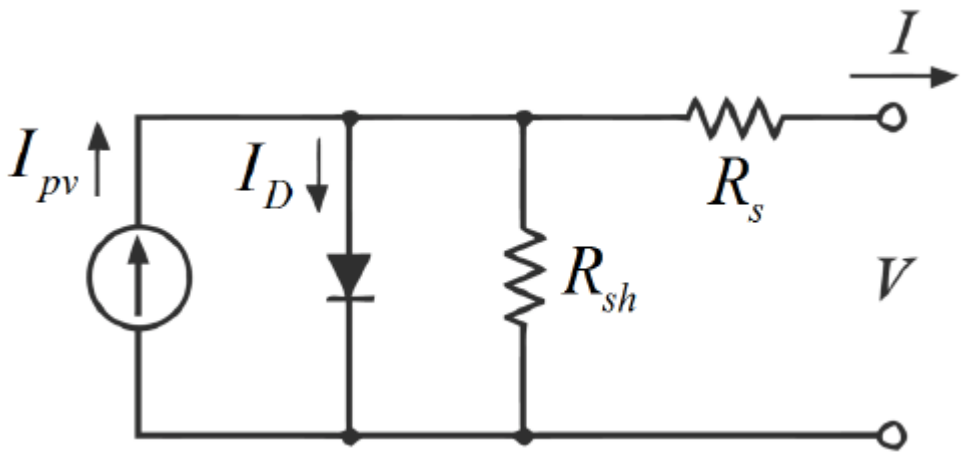

Figure 3.2. Equivalent model of single-diode photovoltaic cell.

In figure 3.2, the photon current IPV is made up of charge carriers that are produced by photon incident. Figure 3.2's PN junction D generates the cell's forward bias voltage and current. Modeling the PV cell as a current source connected in parallel to a diode is an option. As illustrated in figure 3.2, the diode current is ID and the forward voltage is V. A resistance in parallel with the current source is used to mimic the leakage current. As seen in figure 3.2, this is the shunt resistance R_{SH} with current I_{SH} flowing through it. According to [42], there are three factors that contribute to the series resistance Rs shown in Figure 3.2: first, the system current flowing from the cell's emitter to its base; second, the contact resistance between the metal contact and the semiconductor; and third, the top and rear metal contacts. I is the output current of the solar cell, which is the load current [43].

According to Kirchhoff's current law, the output current is given by:

$$I = I_{PV} - I_d - I_{SH} \tag{3.1}$$

By the Shockley diode equation, the current diverted through the diode can be defined as:

$$I_d = I_o \left(e^{\left[\frac{q\,(V+IR_S}{mkT_C}\right]} - 1 \right) \quad (3.2)$$

The current passing through the parallel resistance can be represented by the equation:

$$I_{SH} = \frac{V+IR_S}{R_{SH}} \quad (3.3)$$

The photon current can be represented by the following equation:

$$I_{PV} = [I_{SC} + K_i(T_C - 298)] * \frac{G}{1000} \quad (3.4)$$

$$I = [I_{SC} + K_i(T_C - 298)] * \frac{G}{1000} - I_o \left(e^{\left[\frac{q\,(V+IR_S}{mkT_C}\right]} - 1 \right) - \frac{V+IR_S}{R_{SH}} \quad (3.5)$$

Where:

Ic: is the output current of the PV cell delivered to the load
Iph: is the photon current generated that depends on irradiance quantity
Io: is the dark saturation current of the diode
Id: is the diode current
V: is the output voltage of the PV cell
q: is the electron charge which equals to 1.60217646 ×10-19 C
k: is the Boltzman constant that equals to 1.3806503 × 10-23 J/K
T: is the temperature of the p-n junction in Kelvin
n: is the ideality constant coefficient of the diode
Rs: is the series resistance of the PV cell
Rsh: is the parallel resistance of the PV cell

The renewable energy part of the system contains PV array, MPPT system and boost converter, figure 3.3 shows the main parts of this section.

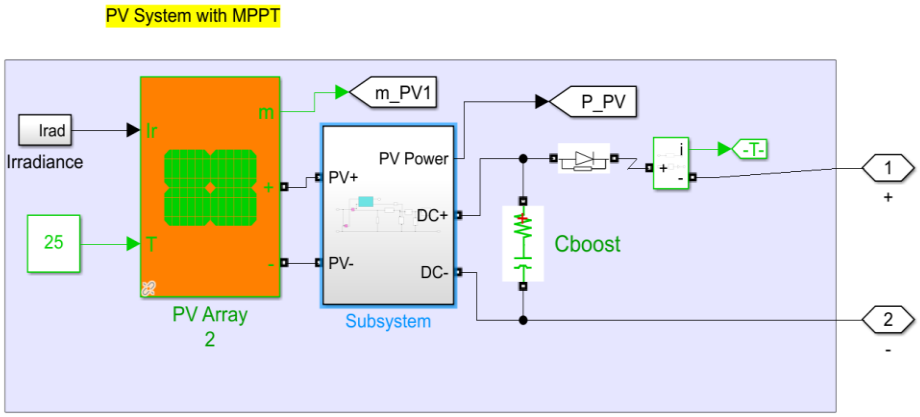

Figure 3.3. Renewable energy source.

In this proposed system, the used solar panel model is Alfa solar P6L60-220 with 45 strings connected in parallel method to create one series module. We can see the Specifications for one module in table 3.1.

Table 3.1. PV module specifications

Item	**Value**
Maximum Power (W)	220.3095
Cells per module (N_{cell})	60
Open circuit voltage V_{oc} (V)	36.35
Short-circuit current I_{sc} (A)	8.39
Voltage at maximum power point V_{mp} (V)	28.95
Current at maximum power point I_{mp} (A)	7.61

P-V & I-V characteristics curves for the used model of PV array in case of; single module and PV array can be showed in figures 3.4 and 3.5. As we see in the bellow figures 3.4 and 3.5, Variations in the PV array's voltage are caused by changing the irradiation level. The current of a PV array is directly associated to the amount of solar radiation, or Iph. Equations (3.1) and (3.2) are representing the photocurrent. The maximum power point drops with lower irradiance levels.

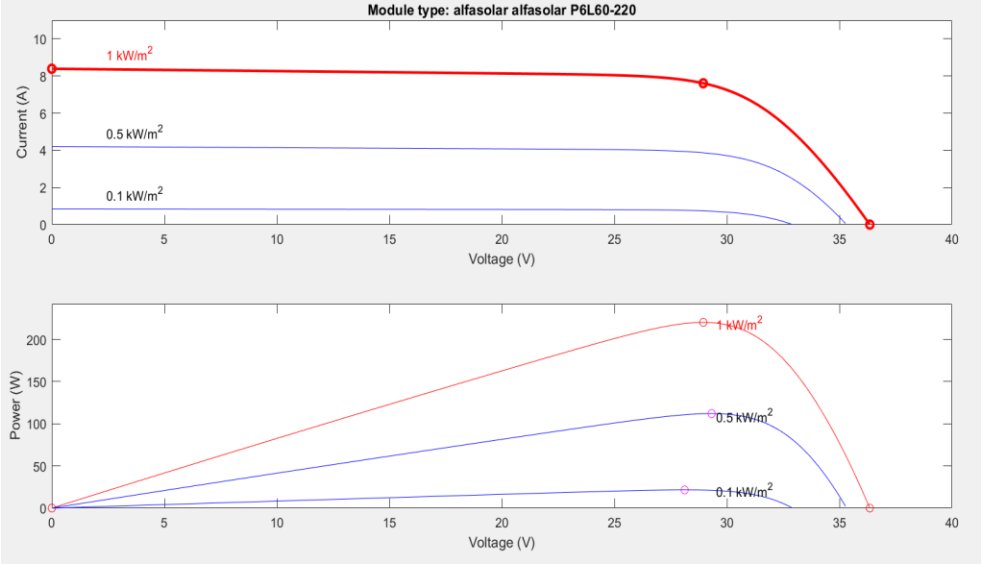

Figure 3.4. P-V & I-V Curves for single module.

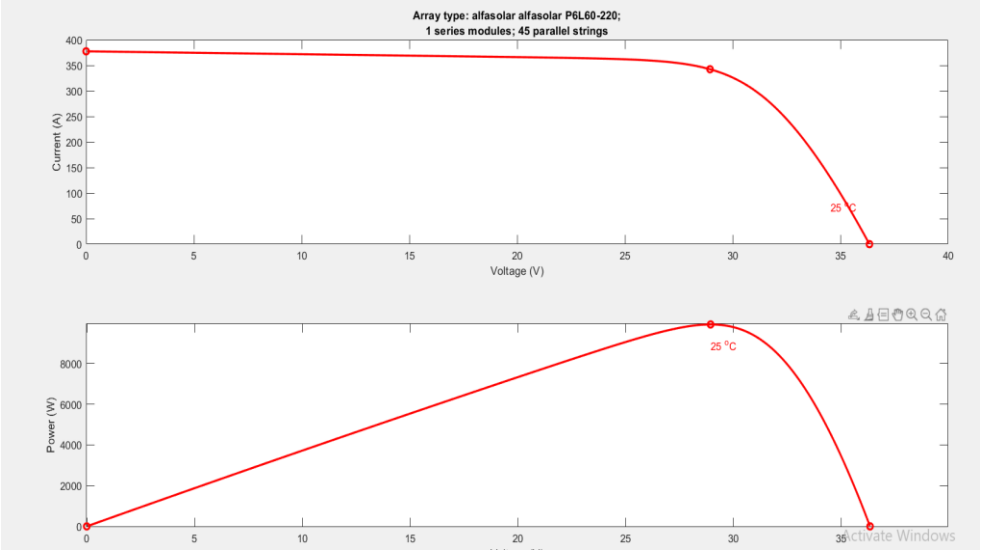

Figure 3.5. P-V & I-V Curves for PV array.

3.3. POWER CONTROLLING OF SOLAR PV SYSTEM

As we have no ability to efficiently connect PV system strings to perilous DC-loads in a straight line because of their nonlinear I-V characteristics. Therefore, PV power controlling system including a DC-DC Boost converter will fulfill two key requirements [44], they have been listed below.

1. Step-up or boost the PV system voltage, manage the PV system through implementing the MPPT technique.
2. Provide a direct output current or voltage or both.

In this work, DC-DC Boost converter will be used as a power controlling system due to the high efficiency & simplicity in work over other power electronic instruments.

3.3.1. Maximum Power Tracking System (MPPT)

Solar radiation on solar panels and solar cell temperature have an impact on characteristic plots, such as P-V and I-V curves. Temperature and solar irradiation changes will cause the MPP to alter. Even on sunny, clear days with abundant of sunshine, solar radiation will fluctuate because the angle at which the sun's rays strike the panel will impact the amount of energy generated. Parallel beams provide almost minimal electricity whereas perpendicular rays offer the solar panels their highest outputThese changes may be fairly significant, particularly during the hottest and coldest parts of the year. Here, power electronics can help to extract the MPP by performing the MPPT duty. The purpose of MPPT is to calculate and compel the solar panel to run at the Vmpp. The Vmpp will alter as temperature and irradiance fluctuate. The operational voltage is pushed toward Vmpp using a DC/DC converter. A different perspective is provided by impedance matching [45], which adjusts the impedance as viewed from the solar panel by altering the input current or voltage of the DC/DC converter to produce a load on the output side of the solar panel. [46].The panel will have the proper voltage or current in accordance with the MPP thanks to this regulated voltage or current.

3.3.2. MPPT Techniques

Through the earlier decades several approaches to obtain the MPP is developed. These methods vary in several features such as, range of effectiveness, required sensors convergence speed, complexity, hardware used for the implementation, cost and correct tracking when irradiance level and/or temperature changes. Among others. Some of the greatest common MPPT methods are listed below [47]:

1. Perturb and observe (P&O) method
2. Incremental Conductance (In Cond) method
3. Fractional open circuit voltage method
4. Fractional short circuit current method
5. Fuzzy logic method

Among numerous methods mentioned above, the two most widely utilized algorithms are the Incremental Conductance (In Cond) and Perturb and Observe (P&O) techniques. Further methods relied on various principles that include fuzzy logic control, current sweep, neural network, and fractional short circuit current or open circuit voltage. The majority of the mentioned methods provide a local maximum as the fractional short circuit current or open circuit voltage, which provides an approximated MPP as opposed to an accurate one. In common cases the P-V curve includes just one maximum. Nevertheless, if the PV panel is partially shaded, there would be a multiple maximum in these curves. Both In Cond and P&O algorithms are relied on the hill-climbing concept that targets to stirring the operation point of the PV panel towards the path wherein the power value goes up. Hill-climbing techniques can be considered as the greatest common MPPT methods because of their ease of implementation when the radiation level is constant and their good performance [48]. The simplicity and cheap processing power requirements of the two approaches are benefits. The drawbacks, however, include vibrations that surround the MPP and lead them to get disoriented as well as tracking the MPP in the wrong direction due to quickly changing atmospheric conditions. In this thesis, we used P&O technique.

3.3.3. Perturb and Observe (P&O)

This section explains the perturb and observe (P&O) algorithm, which is popular because it is straightforward to build and uses fewer computer resources than more sophisticated algorithms. Figure 3.6 shows the P&O algorithm's logic flow diagram. By comparing the output power at two successive measuring locations, P&O controls the PV array's current or voltage. To do this, a DC/DC converter or an inverter's duty cycle is used to continuously adjust the regulators' voltage or current set points, and the output power is compared to that of the preceding sample. Because of this, the procedure is known as perturbs and observe. It will continue to change the converter's current and voltage set points in the same orientation until the new power is lower than the previous one. The MPP is subject to change because the algorithm has no means of knowing when it has arrived at it, and it will alter as the weather changes. The duty cycle will continue to fluctuate, and the shift will be noticeable. Consider, for instance, that the voltage at the left of the MPP of the curve in figure 3.7 corresponds to the duty cycle of the converter. The algorithm will determine the direction for the next perturbations after changing the duty cycle to achieve a higher input voltage, computing the new power, and comparing it to the prior power. If the power is greater at the new location than it was at the original location, the perturbation was made in the right direction, and the duty cycle will be adjusted to move the input voltage in the same path as previously. This will keep happening until the comparison power drops below the prior one. As the set point will be to the right of the MPP in this instance, changing the duty cycle will result in a decrease in input voltage. At this time, the algorithm will begin to oscillate around the MPP, as shown in figure 3.7. As a result, the MPP will continue to behave in this way and never become stable. The minimal computational requirements for P&O implementation are a significant benefit. Even with constant sun radiation, the drawback is that the real MPP is never truly attained. To get the most out of the solar panel's available power, the P&O MPPT technique is applied. It is dependent on the variability in PV-produced power as the voltage changes. As a result, the controller modifies the PV voltage step-size in the same direction when $dP/dV > 0$. If not, the MPPT controller changes the direction of the voltage step until the MPP [49].

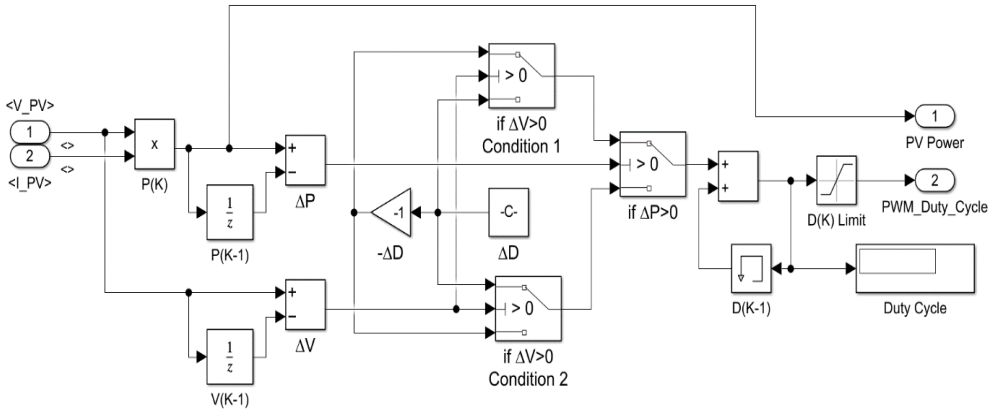

Figure 3.6. MPPT P&O algorithm.

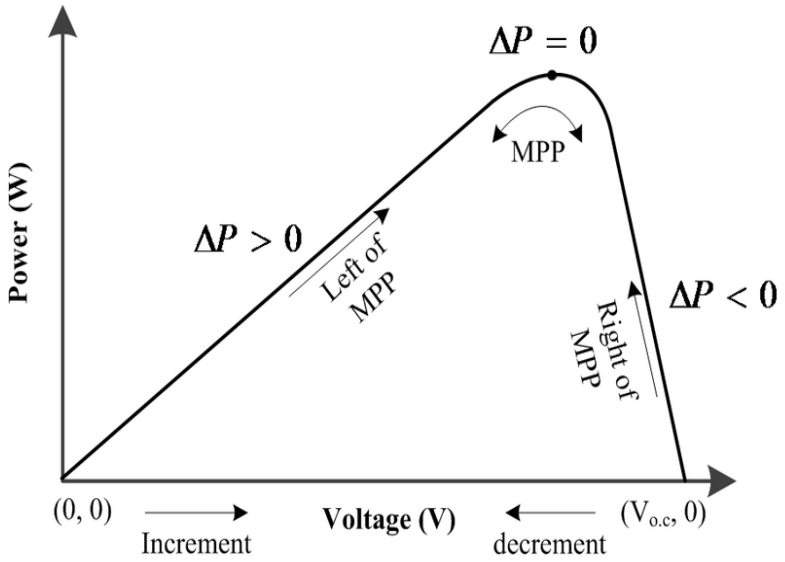

Figure 3.7. P&O MPPT working curve

3.3.4. Boost Converter

The conversion of a fixed-input DC voltage to a changeable DC voltage is required for several technical applications. A DC-DC converter, as well known as a DC Converter, converts voltage directly from low level DC to high level DC. An AC transformer with a changeable turn's ratio can be compared to a DC converter. As a transformer, there is a possibility to use it as a step up or step-down DC voltage source.

In general, DC converters can be used to control tracing motors in electric vehicles, mine hauler, marine hoists, forklift trucks, and trolley cars. They are highly efficient,

have a quick dynamic response and have good acceleration control. They can also be utilized to brake DC motors generatively, returning energy to the power source. So, this feature saves energy in transport systems with repeated steps. Furthermore, DC converters are also employed in DC voltage regulators and to provide a DC current source, particularly for current source inverters, by coupling them with an inductor. [50]. Figure 3.8 displays the functional block diagram for the boost converter.

Boost converter output voltage is given by equation 3.6 (neglecting the voltage drop across the circuit elements):

$$V_{out} = \frac{V_{in}}{1-D} \tag{3.6}$$

V_{out}: output voltage.
V_{in}: input voltage.
D: duty cycle of switching.

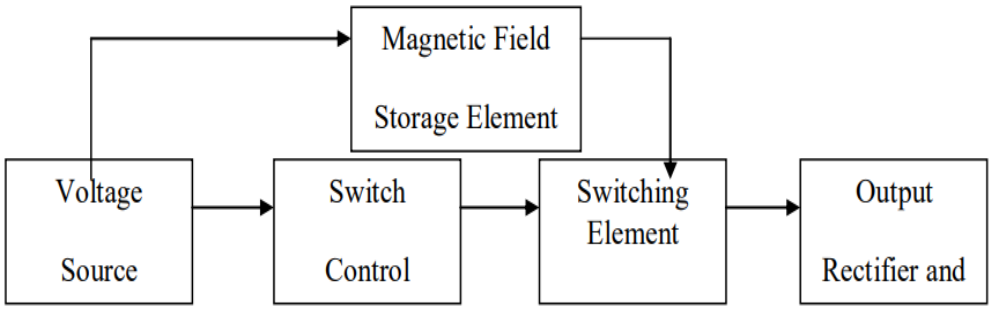

Figure 3.8. Boost converter block diagram.

As a result, the output voltage is straightly proportional to the duty cycle, as is quite obvious. The circuit diagram for a boost converter is shown in figure 3.9 that consists of Inductor, capacitor, diode and IGBT Switch. The decision of what kind of inductor to use is the certain obstacle in converter design. The ripple current and inductance are inversely proportional. As a result, a larger inductor must be used so as to reduce the ripple [51].

To convert the PV array voltage into that level to attain the maximum power point MPP, a type of DC-DC boost converter is used. The boost converter main switch

(IGBT) is triggered by using PWM DC-DC controller. Depending on the PV array's operational circumstances, the P&O method generates the controller duty cycle. The PWM switches at a frequency of 5000 Hz. Figure 3.9 shows the boost converter

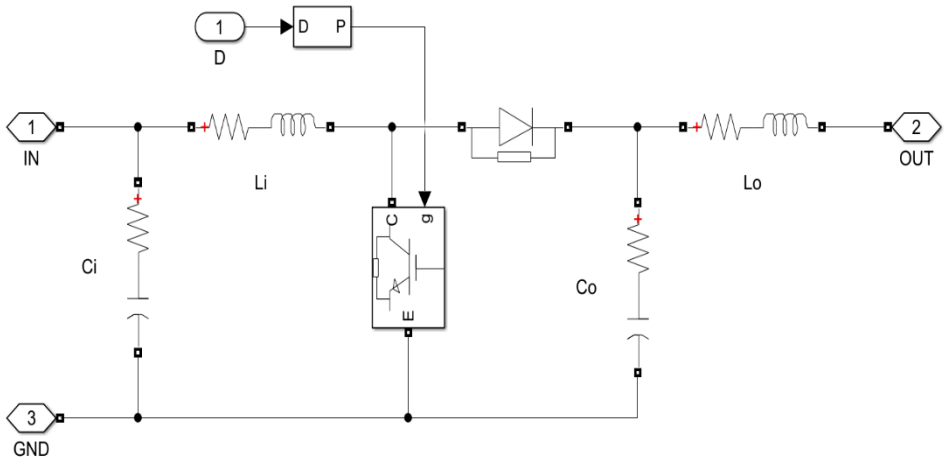

Figure 3.9. Boost converter.

3.3.5. Buck Converter

The greatest fundamental SMPS topology is a buck converter. Typically, it is employed in manufacturing to transform a higher input voltage to a lower output voltage. The Galvanic isolation between the input and the output is not maintained since the buck converter is not isolated. Figure 3.10 shows the buck converter, it is regarded as the most widely utilized design for dispensing power in the most complex systems, like broadband communication boards and server motherboards [52]. It obtains the necessary local voltage level from a higher voltage bus that is shared by a lot of the system's converters. A buck converter itself is made up of one active switch controlled by an integrated circuit, filter elements and a rectifier. This simplicity of utilization and cost-effective enables high-efficiency power distribution across the application.

The filter inductor on the buck converter's output side sends to the load a horizontal, constant output current waveform. And while this may be viewed as a qualitative benefit, it requires for specific regard when dealing with large load transients. Buck converter output voltage given in equation 3.7.

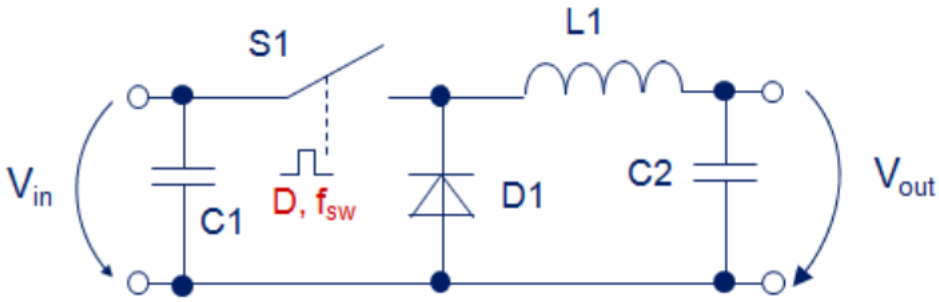

Figure 3.10. Buck converter general circuit diagram.

$$V_{out} = D \times V_{in} \tag{3.7}$$

Where:

V_{out}: output voltage.
V_{in}: input voltage.
D: duty cycle of switching.

3.4. ENERGY STORGAGE SYSTEM (ESS)

Because of being the nature of renewable energy resources is intermittent and with the purpose of compensating the times when the generation of sunlight is low or nonexistent, energy storage systems are regarded as crucial components. The power storage system essentially contains a battery and battery charging controller as shown in figure 3.11. Solar photovoltaic systems are used with a power storage system to minimize the uncertainty surrounding the local availability of renewable energy sources. [53]. When there isn't enough generation or when demand is high, the battery system's stored energy could be invested to generate the necessary power. The energy storage system will enhance the dependability and stability of the microgrid power systems by reducing the effects of power fluctuation caused by the installed renewable energy sources. The battery's effectiveness and performance are influenced by the environment's temperature, charge level, voltage impacts, and pace of charging and discharging. These parameters also affect how long a battery lasts. However, depending on the battery used, these parameters have different effects. Lithium-ion batteries are utilized in this study because to their lifespan cost, durability, safety and

high efficiency benefits over other kinds of batteries. In order the battery remain durable, it must not be overcharged because doing so would reduce the battery's effectiveness and shorten its lifespan. Likewise, the battery should not be over discharged because doing so would shorten the battery's lifespan. A fundamental need for the battery's durability is that its maximum State of Charge (SoC) must be set to its nominal capacity. Moreover, the battery's SoC should not be less than 30% at all times [54].

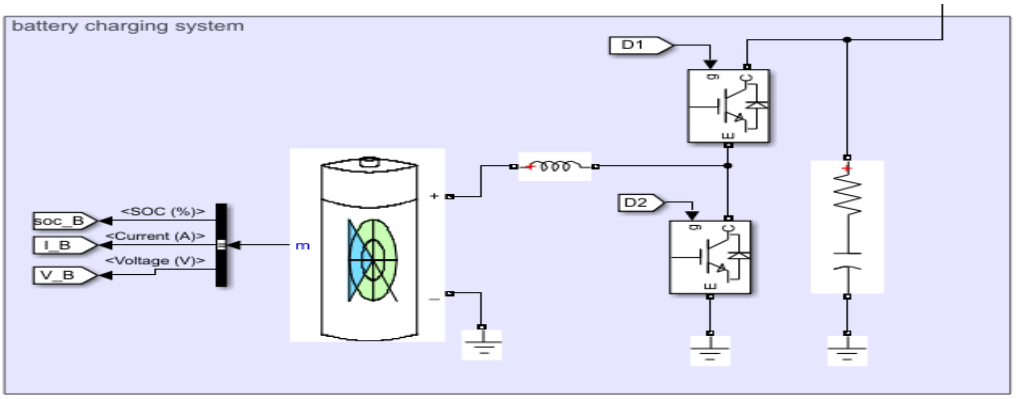

Figure 3.11. Energy storage system.

3.4.1. Battery Charging Controller

Charge controllers are employed in microgrid systems to govern the flow of current to and from the battery bank [55]. They are essential to maintain the DC bus voltage and safeguard the batteries. In this DC thesis, in order to feed power to the microgrid from the batteries when the PV output is lower than the demand, the charge controller will turn on a bidirectional converter. As demanded by the battery bank system, the bidirectional converter will minimize the PV output voltage generated. Figure 3.12 depicts the suggested logic for the DC microgrid system's battery charging controller. The majority of battery systems are made to work between 30 and 90% of their capacity. Because of this, the logic process in the controller will determine whether the batteries are between 30 and 90% charged, and if so, based on the balance of power quantity between generation and consumption, the batteries can either go through charging or discharging. The batteries will be charged when the battery systems have a low SOC of less than 30% and when the quantity of power produced exceeds the

necessary load, however if the load exceeds the power produced and the battery bank has a high SOC of more than 30%, the battery bank will go through discharging mode. Load shedding has to be taken into consideration to protect the batteries. The final scenario is when the batteries have a high SOC of more than 90% and to prevent overcharging of the batteries and an increase in the DC bus voltage, current will be delivered to a dump load, this scenario happens in case the microgrid is producing more energy than it needs. The battery charging controller will manage the bidirectional buck-boost converter, the control process contains two loops (voltage loop and current loop), in the voltage loop, a comparison is done between the bus voltage and the reference voltage to obtain the battery reference current which will be compared with battery current in current loop to obtain battery behavior. Two PI controllers are used in charging and discharging process control system.

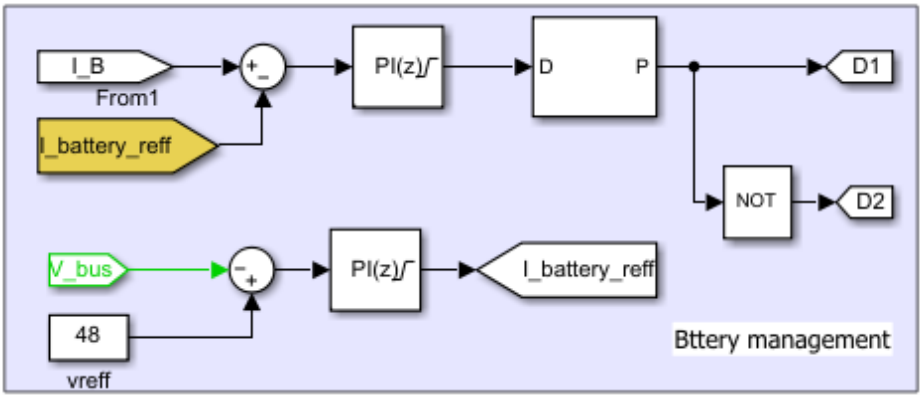

Figure 3.12. Proposed logic for battery charge controller.

3.4.2. Bidirectional Converter

To enable power to flow to and from the batteries in the microgrid systems, a bidirectional converter is necessary. Bidirectional power flow is not possible with the classic buck and boost converters. This is due to the fact that each one of them incorporates a diode to prevent the flow of reverse current. By integrating the characteristics of buck and boost converters and swapping their diodes with switches, as shown in figure 3.13, a bidirectional converter can be created. The converter can be utilized as a boost converter by employing the bottom switch to supply power from the low-voltage end to the high-voltage end, or it can be utilized as a buck converter by transmitting power from the high-voltage end to the low- voltage end through

employing the top switch. In the purpose of minimizing the challenges of produced power instability from renewables and to maintain voltage, the charge controller will operate the bi-directional switch, determining whether power should be delivered to or from the battery. [56].

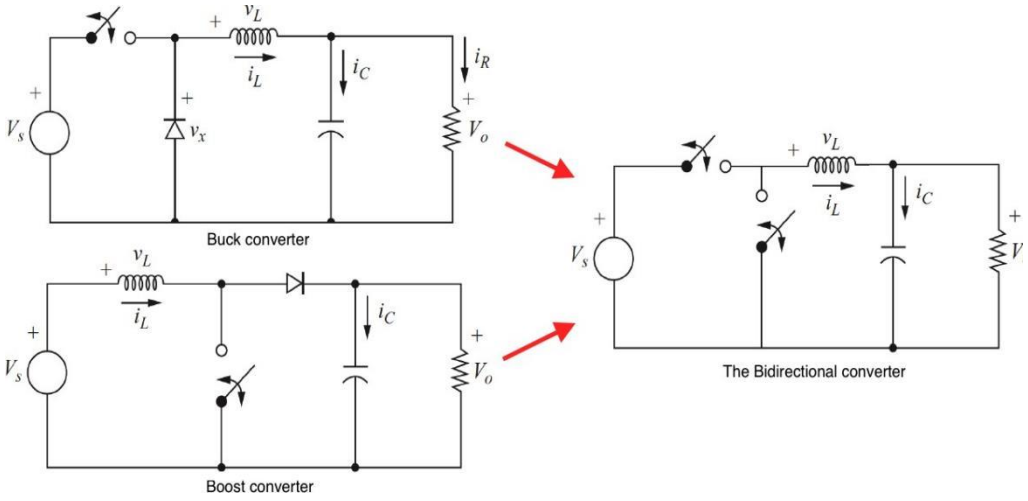

Figure 3.13. Bidirectional converter.

3.4.3. PI Controller

Voltage-based droop control or communication-based management are two ways to manage a microgrid [57]. In this thesis, we'll employ a proportional-integral (PI) controller and the communication-based control approach. The charge controller's control mechanism will be a PI controller. The error e (t) between the output y (t) and the preferred set point Ref is calculated using this regularly employed control technique. The error signal is corrected proportionally and integrally, and the sum of these adjustments creates the control variable u (t). So, this mentioned control variable is utilized to lower system error, and the procedure is continued to do so. The monitored output y (t) in the DC microgrid scheme will reflect the DC bus voltage, with the reference being the target DC voltage of 48 V. The control variable u (t) shall run the bidirectional converter so as to conserve the DC bus voltage, which will regulate the flow of power between the microgrid and battery batteries. In relation to the error, the proportional term produces a proportionate reaction. A proportional only controller would not activate the bidirectional converter if there was no error signal, and once a zero steady state error was obtained, the system's inertia would cause the

DC voltage to diverge. As a result, we also employ an integral response that incorporates a control depending on prior errors. Although a PI controller will respond more quickly, it has good power regulation and zero steady-state error. [58]. In this thesis, a voltage-based droop control is used to managing the power in system.

3.5. DC BUS SYSTEM

DC bus contains both DC loads and AC load. The DC load is supposed to be resistive load with total capacity of 5 KW connected directly to the DC coupling bus system. The AC load is coupled to the DC coupling bus system through a full bridge single phase and set up transformer with total capacity of 5KW.So, the total loads associated to the bus system is 10KW. The DC bus voltage is considered to 48 be VDC as default value. There is no way to add actual power to the utility network since the DC coupling bus system is interconnected to the main utility grid using a full bridge uncontrolled rectifier. When the PV system's output is bigger than what is required by the load, the extra energy is stored using battery banks. When the amount of power produced by the PV system is insufficient to meet the load claim, the storage system will provide the necessary power to the load. Figure 3.14 shows the DC bus and the rectifier.

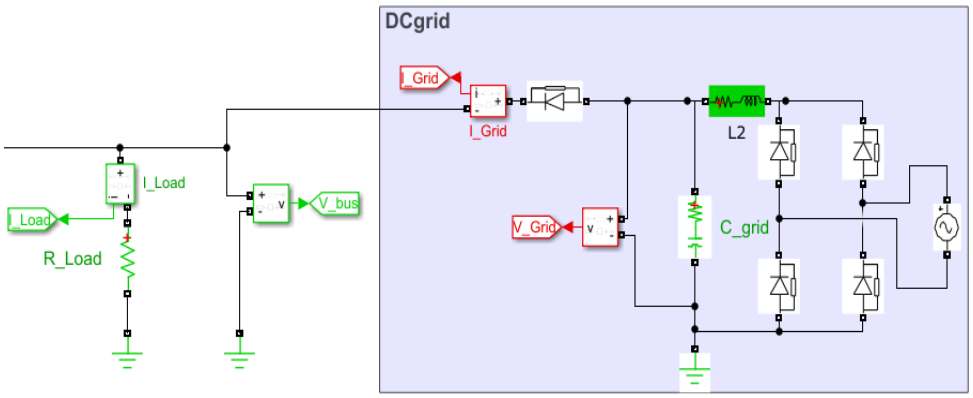

Figure 3.14. DC microgrid.

3.5.1. Uncontrolled Bridge Rectifier

Depending on the application, uncontrolled rectifiers might be single- or three-phase. So, in our work the used rectifier is a single-phase uncontrolled full bridge rectifier. The selection of this type of rectifiers depends on the proposed system operation, here

is no power injection to the utility network (the utility grid to the load is the sole direction in which energy flows.). Figure 3.15 shows the rectifier. The voltage output of the uncontrolled full bridge rectifier is given in equation 3.8. Figure 3.16 displays the rectifier's output waveform.

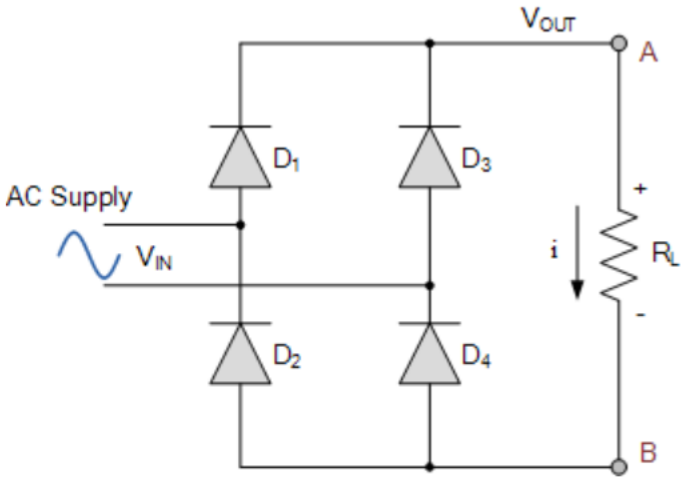

Figure 3.15. Full bridge uncontrolled rectifier.

$$V_{dc} = \frac{2V_{max}}{\pi} \tag{3.8}$$

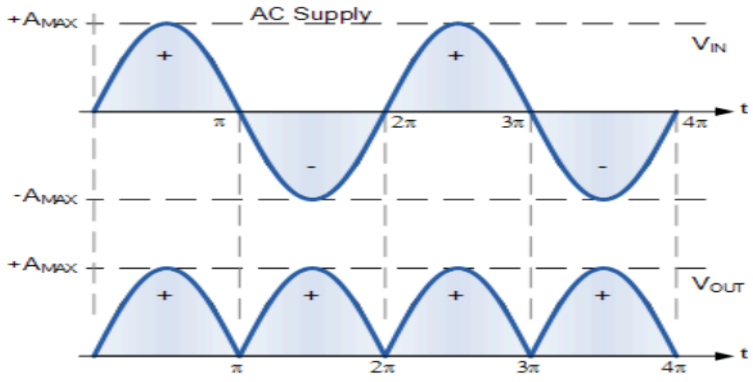

Figure 3.16. Rectifier output.

3.6. SYSTEM LOADS

3.6.1. AC load

The AC load is connected to the DC microgrid using a full bridge single phase inverter and step-up transformer, the load active power is set to be 5KW. Figure 3.17 shows the AC load part of the proposed system.

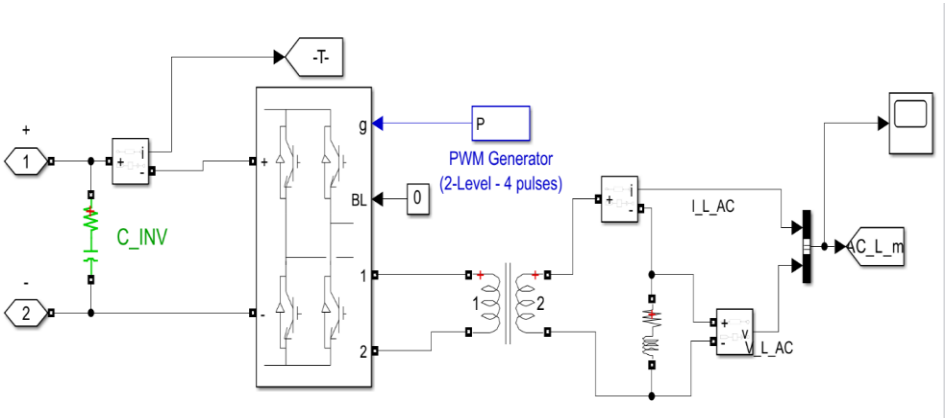

Figure 3.17. AC load circuit.

3.6.2. DC Load

The DC load assumed to be a resistive load connected directly to the DC microgrid. The power of the DC load is also 5KW. Figure 3.18 shows the DC load part of the proposed system.

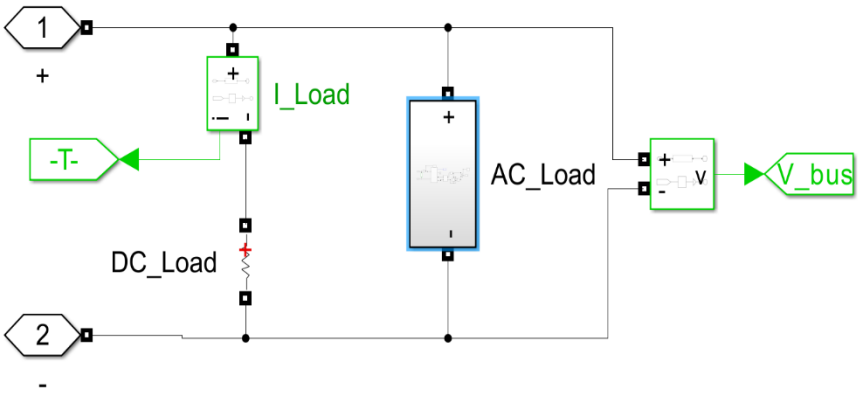

Figure 3.18. DC load part.

3.6.3. Load Sharing

The load sharing depends on the quantity of real power produced by the PV array system. The power flow depends on the DC-bus voltage which is the deference between the voltage generated by PV system after being boosted by the DC-DC converter and the full bridge uncontrolled rectifier DC output voltage. Figure 3.19 shows the algorithm of load sharing process.

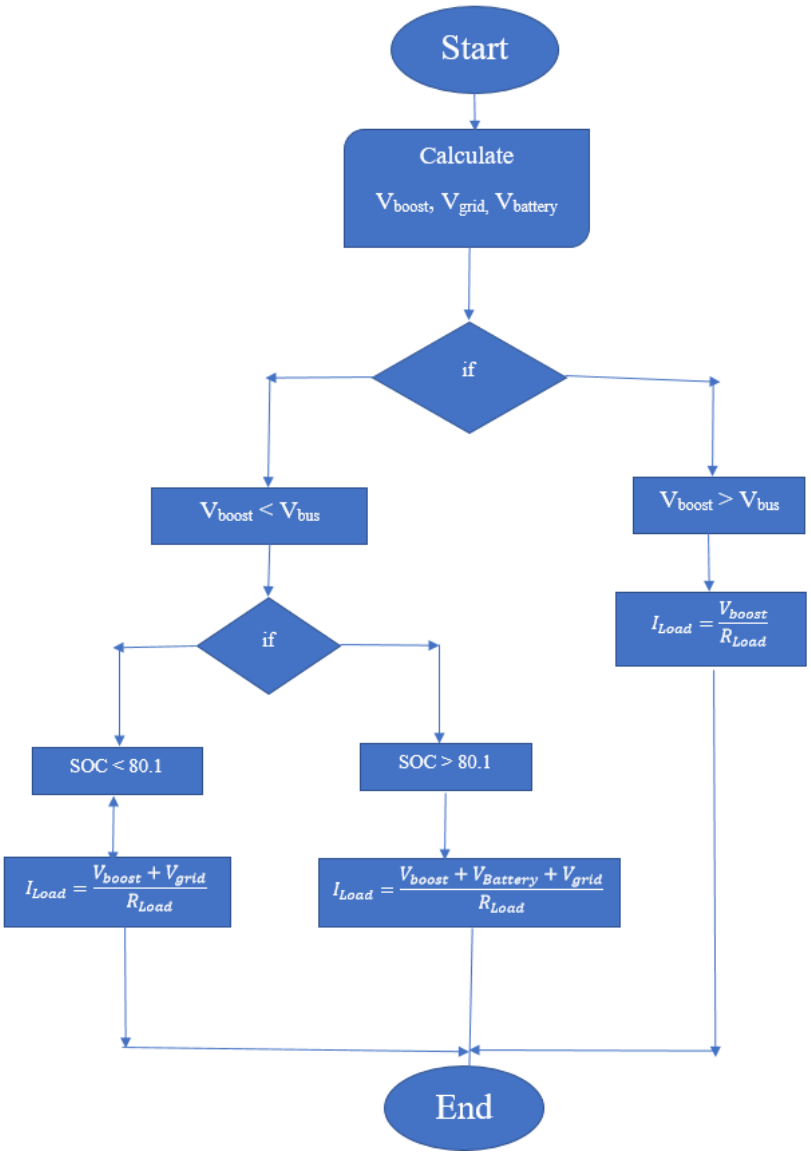

Figure 3.19. Load sharing algorithm flow chart.

PART 4

RESULTS AND DISCUSSION

A PV array with a total capacity of 10 KW is considered here to power a typical 10 KW of AC & DC loads. DC loads with capacity of 5 KW are coupled directly to the DC bus system. While, AC loads with capacity equal to the DC loads are associated to the DC bus system using a full bridge single phase inverter and step-up transformer. The simulation results for the DC microgrid system are discussed here in this section. Results are recorded under different irradiation levels and load capacities. Irradiation levels is considered to be 0 KW, 250 KW, 500 KW, 750 KW & 1000 KW. While, load capacities are considered to be 25 % of full load, 50 % of full load & 100 % of full load.

4.1. SYSTEM SIMULATION RESULTS UNDER THE CHANGE OF BOTH LOAD AND IRRADIANCE

In this section the system is simulated for many cases of load and real power production.

4.1.1. Case 1: 250 W/m^2 Solar Radiation and 25% full Load

In this case, irradiation level is considered to be 250 W/ m2. While, 25 % capacity of the system loads is coupled to the system bus. Figure 4.1 shows the system voltages for this case. The bus voltage is in the desired range about 48 VDC.

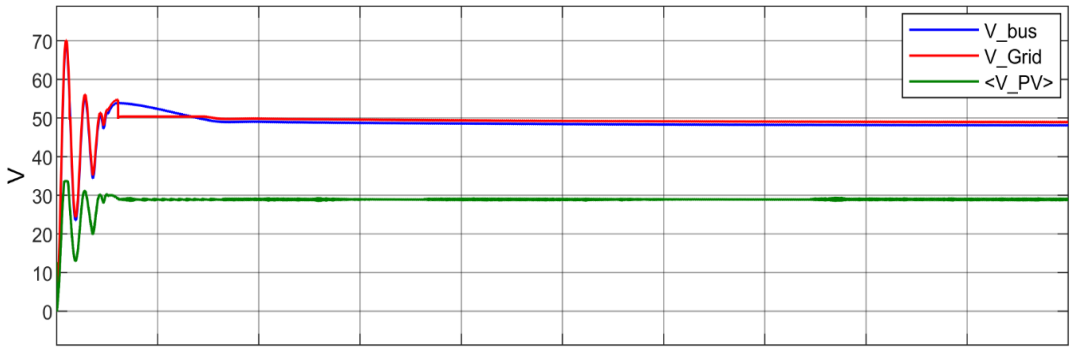

Figure 4.1. System voltages in case of 250 W/m2 radiation level and 25% full load.

The system currents are shown in figure 4.2, as we can see that the grid current is zero in this case and that means the grid is not delivering any real power to the load. While, the battery current is in minus range and that means the battery is in charging mode. The PV array power in this case is about 2500 watt that means the MPPT system has a high performance. The power and irradiance curves are shown in figure 4.3.

The system power curves are shown in figure 4.4, the grid does not supply any real power to the load.

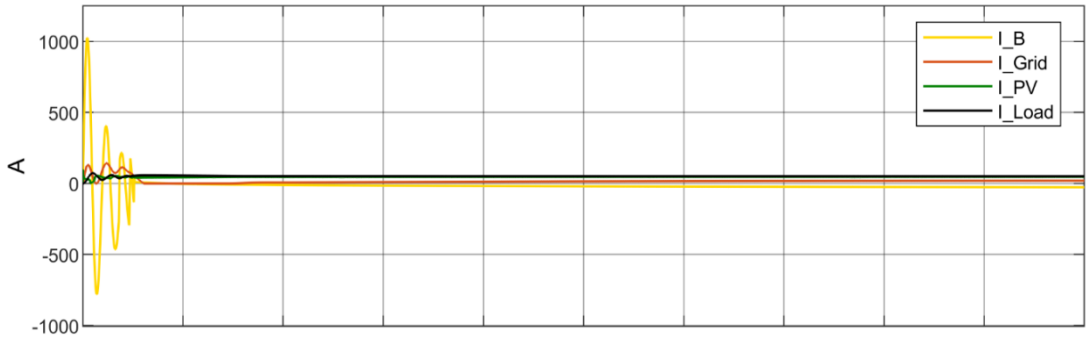

Figure 4.2. System currents in case of 250 W/m2 and 25% full load.

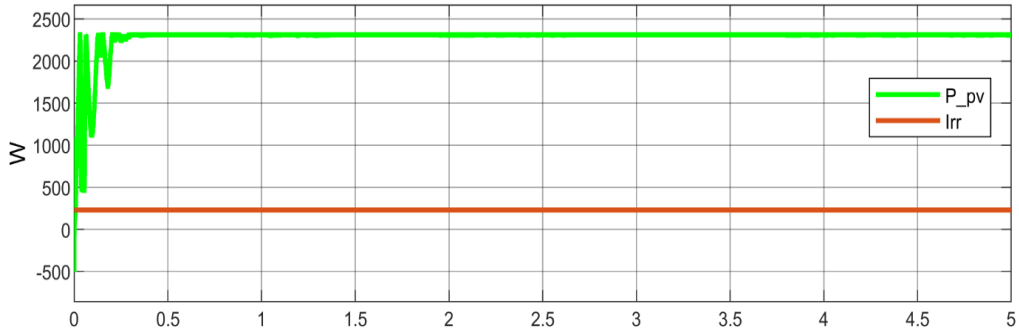

Figure 4.3. PV power and irradiance curves.

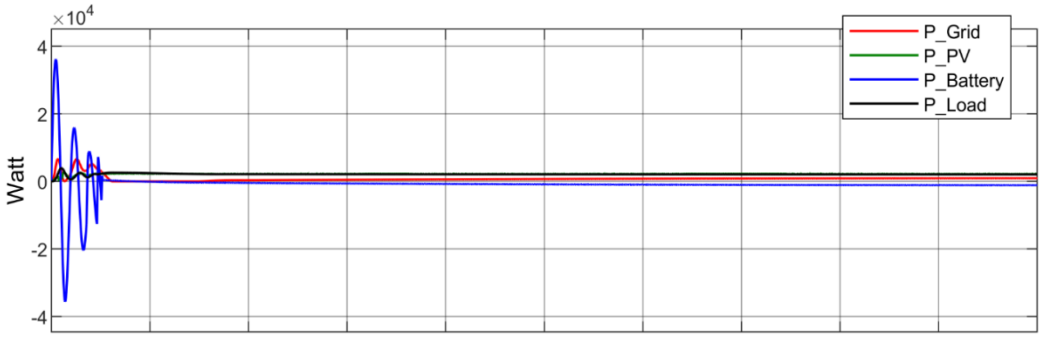

Figure 4.4. System power curves in case of 250 W/m2 and 25% full load.

Lastly, the state of charge curve of battery is displayed in figure 4.5. As we see, power generated by the PV system is 2.5 KW. While, the system loads connected to the bus is also 2.5 KW. So, PV system powers the total loads and the battery and grid system do not share in feeding the loads.

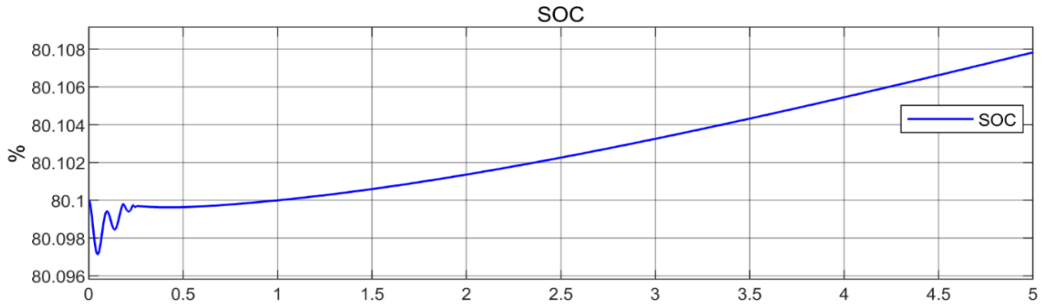

Figure 4.5. Battery state of charge curve.

4.1.2. Case 2: 250 W/m^2 Solar Radiation and 50% Full Load

In this case, the system is half loaded, the total loads are about 5000 watts. The irradiance is considered to be 250 W/m^2. The system voltage curves are displayed in figure 4.6. In this case the bus voltage is in the desired range about 48 VDC.

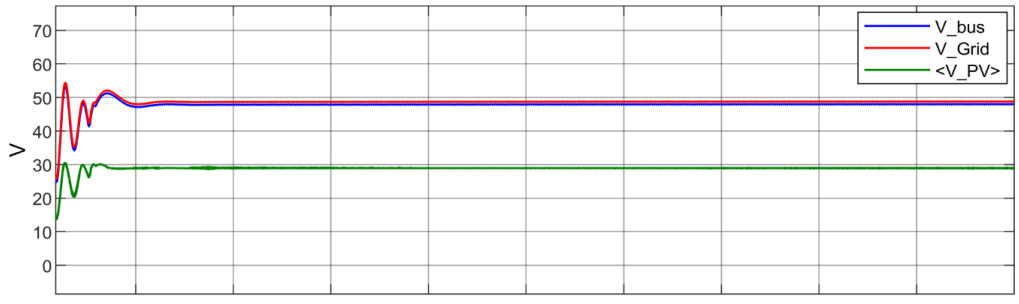

Figure 4.6. System voltage curves in case of 250 W/m2 and 50% full load.

System current curves are presented in figure 4.7. While figure 4.8, shows the PV array power curve.

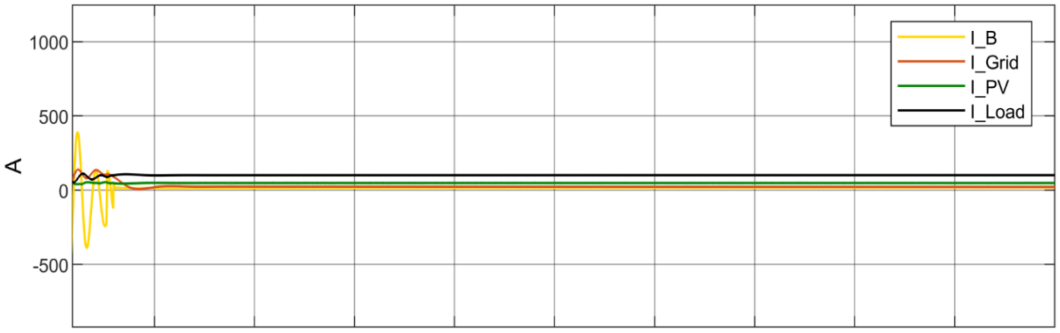

Figure 4.7. System curves in case of 250 w/m2 and 50% full load.

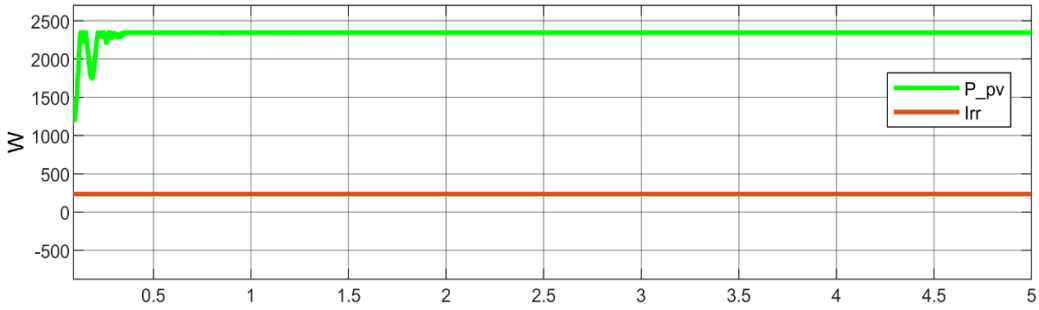

Figure 4.8. PV array power curve.

System power curves are presented in figure 4.9, while figure 4.10 displays the MPPT performance in this case.

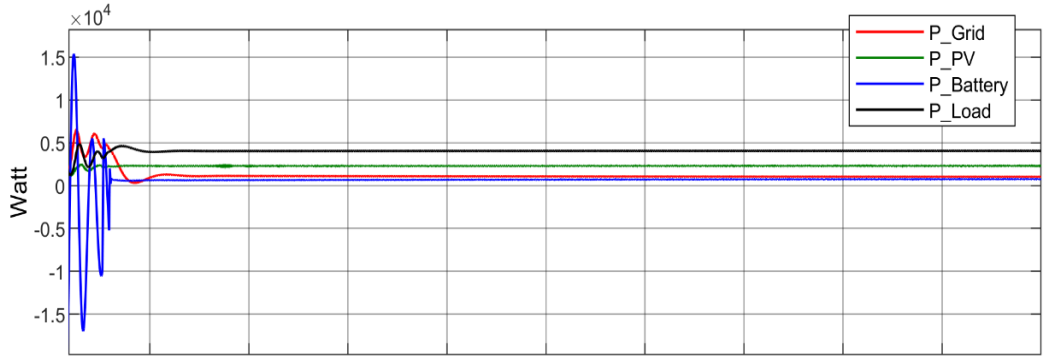

Figure 4.9. System power curves in case of 250 W/m2 and 50% full load.

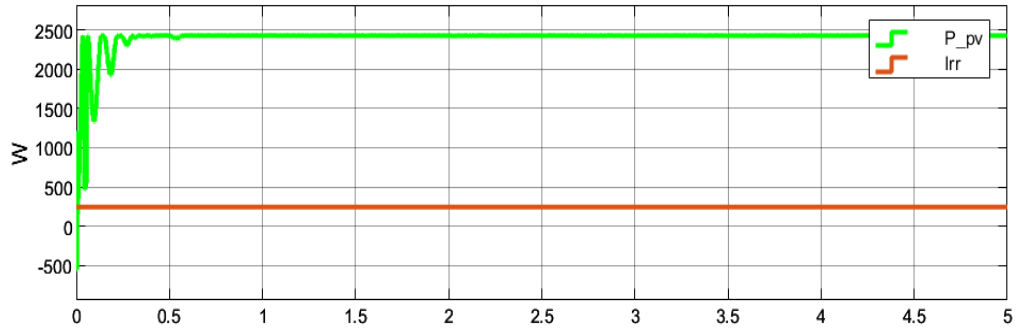

Figure 4.10. MPPT performance in case of 250 W/m2.

4.1.3. Case 3: 250 W/m^2 Solar Radiation and Full Load

In this case, the system is full loaded. Load power for both AC and DC loads are 10 KW. Figure 4.11 shows the system voltage curves in this case, figure 4.12 shows system current curves for the same case respectively.

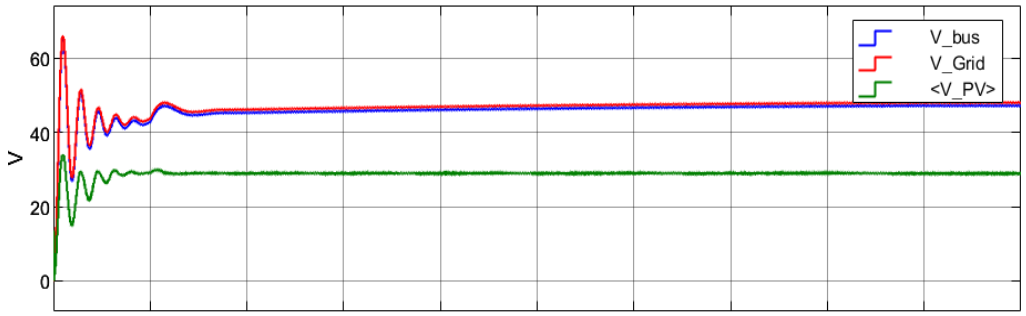

Figure 4.11. System Voltage curves in case of 250 W/m2 and full load.

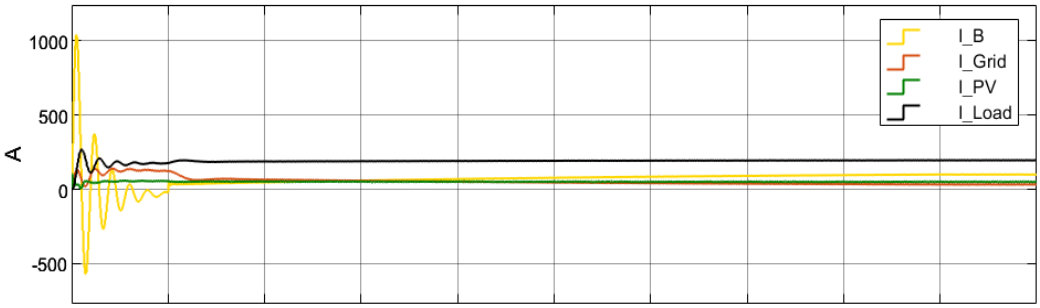

Figure 4.12. System current curves in case of 250 w/m2 and full load.

The MPPT system is still tracking the maximum power point. As we see in figure 4.13 the total amount of produced power in this case is about 2500 watt.

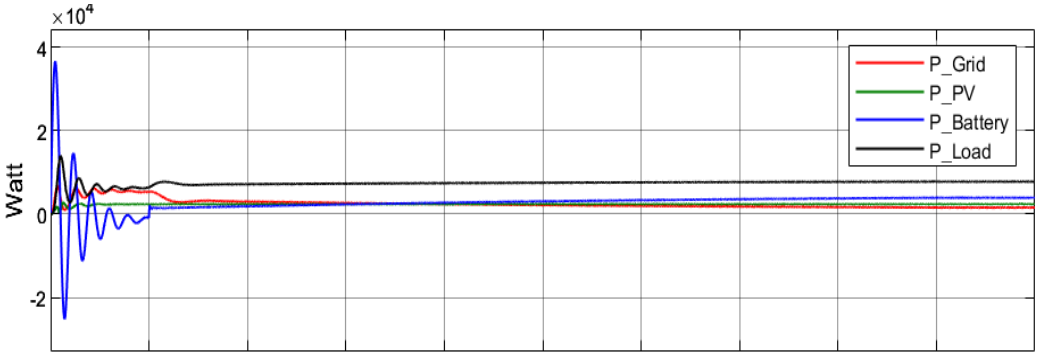

Figure 4.13. System power curves in case of 250 w/m2 and full load.

While battery SOC curve is shown in figure 4.14. As we see in this case, PV system produces only 2.5 KW. While, the total capacity of loads coupled to the DC bus is 10 KW. So, PV system powers only 25 % of the load and battery and national grid power the rest 75 % of the system loads.

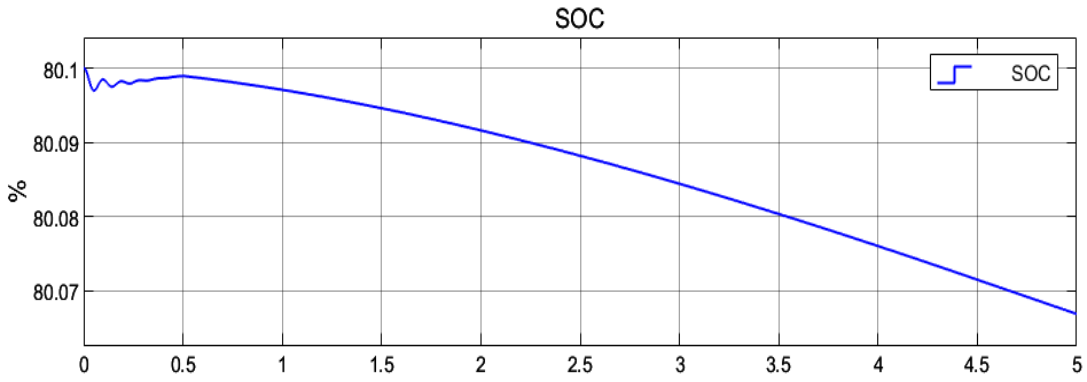

Figure 4.14. Battery SOC curve in case of 250 w/m2 and full load.

4.1.4. Case 4: 500 W/m^2 Solar Radiation and 25% full Load

In this case, the PV array produces 5000 watts when the radiation level is 500 W/m^2. 25 % capacity of the system loads are coupled to the bus system. System Current curves for this case are presented in figure 4.15, and system voltage curves are presented in figure 4.16.

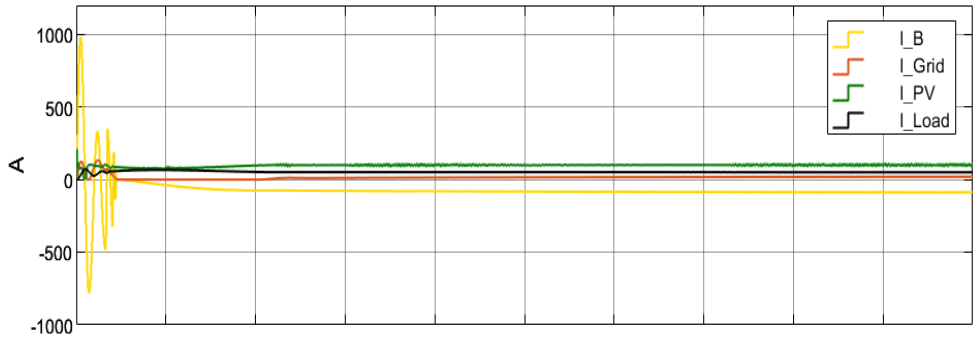

Figure 4.15. System current curves in case of 500 W/m2 and 25% full load.

As we see in this case, PV system produces 5 KW real power. And, the total capacity of DC & AC loads connected to the DC bus is 2.5 KW. Figure 4.17 shows the PV array power curve with irradiance level of the system. While, figure 4.18 shows System power curves, which shows that the PV array supplies the total loads and also charges the battery while the grid is not sharing in the feeding process.

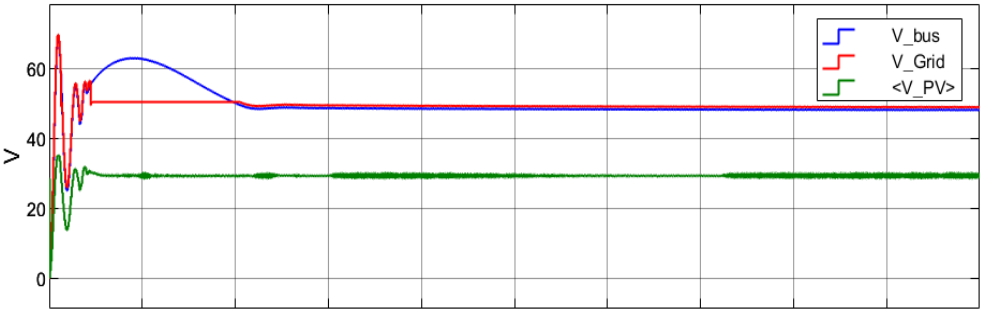

Figure 4.16. System voltage curves in case of 500 W/m2 and 25% full load.

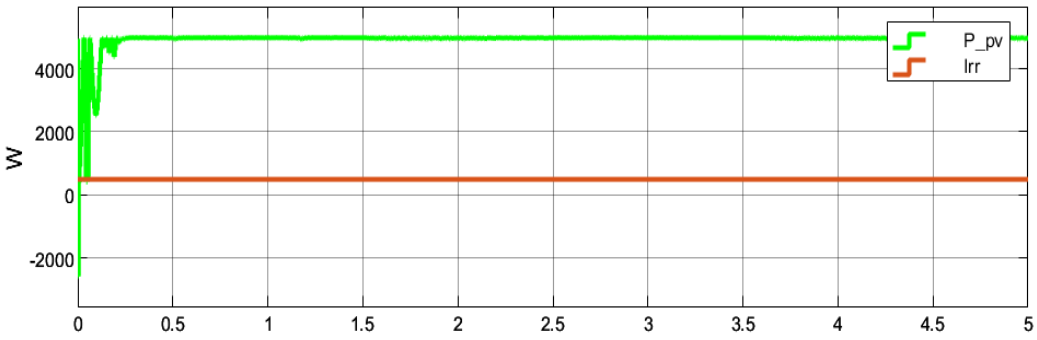

Figure 4.17. MPPT performance in case of 500 W/m2.

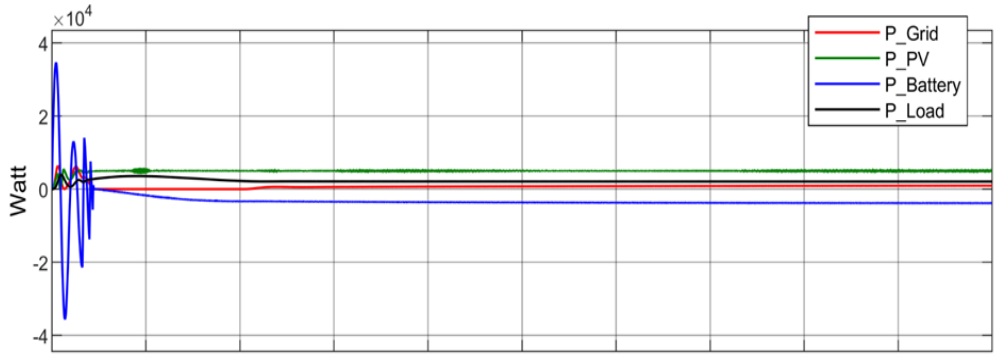

Figure 4.18. System power curves in case of 500 W/m2 and 25% full load.

The battery SOC curve is shown in figure 4.19, which shows that the battery is in charging state.

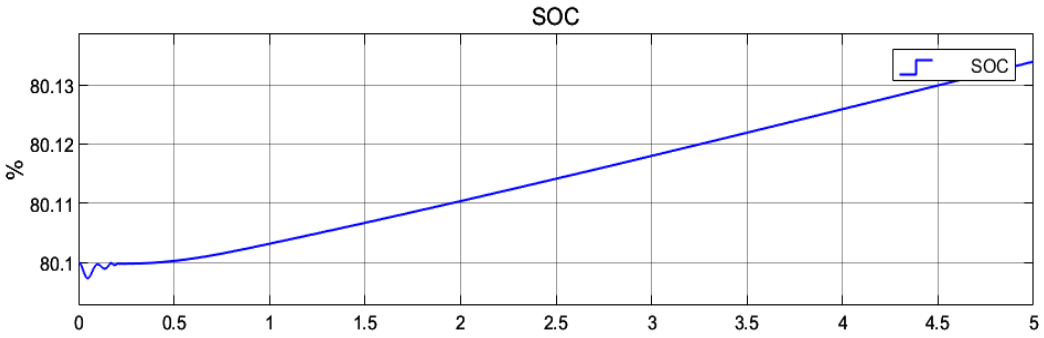

Figure 4.19. Battery SOC curve in case of 500 W/m2 and 25% full load.

4.1.5. Case 5: 500 W/m^2 Solar Radiation and 50% full Load

In this case, radiation level is considered to be 500 W/ m2. While, half capacity of the system loads is coupled to the system bus. Figure 4.20 displays the system current curves for this case and figure 4.21 shows the system voltage curves for the same case. The PV system power curve and irradiance level curve are presented in figure 4.22, the PV power curve is plotted for each case to show if the MPPT algorithm is working in the required performance. Figure 4.23 displays the power curves of the system Power in case of 500 W/m^2 and 50% of the full load. Battery SOC curve is displayed in figure 4.24.

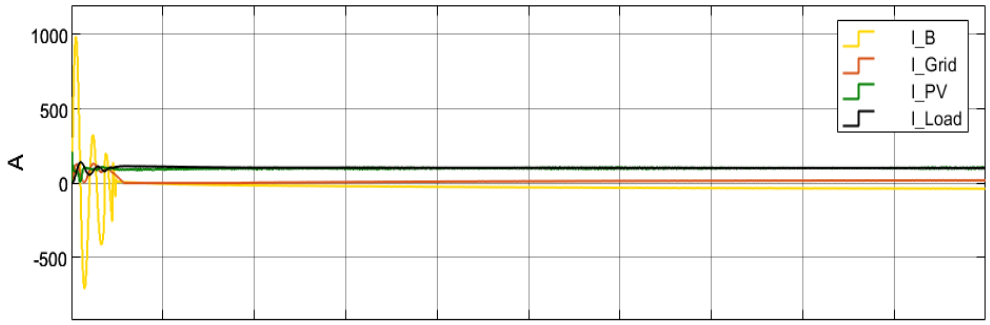

Figure 4.20. System current curves in case of 500 W/m2 and 50% full load

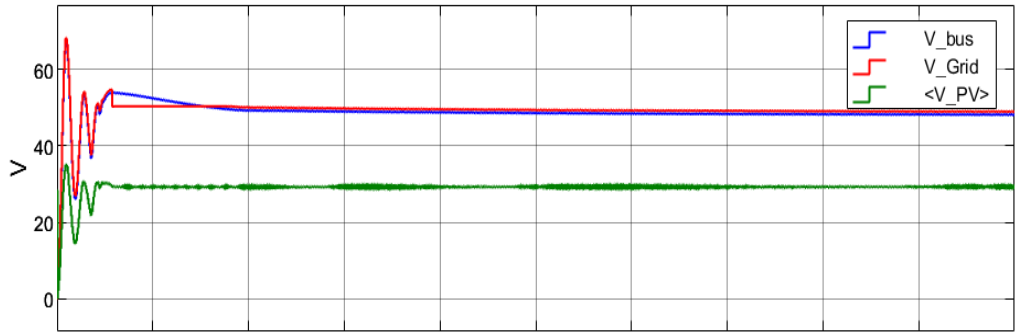

Figure 4.21. System voltage curves in case of 500 W/m2 and 50% full load.

As we see in this case, PV system produces 5 KW real power. And, the total capacity of DC & AC loads coupled to the DC bus is also 5 KW. So, PV system powers 100 % of the loads and battery and national grid do not share in feeding the loads. The generated real power is more rather than the load real power and that means the battery is in charging mode.

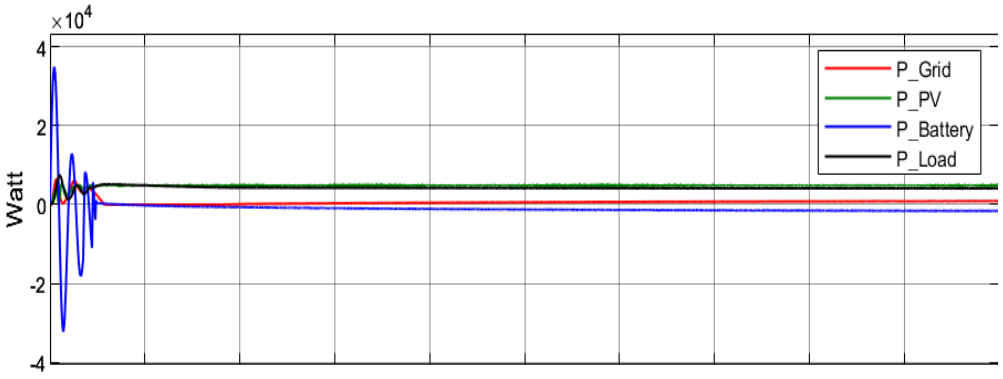

Figure 4.22. System power curves in case of 500 w/m2 and 50% full load.

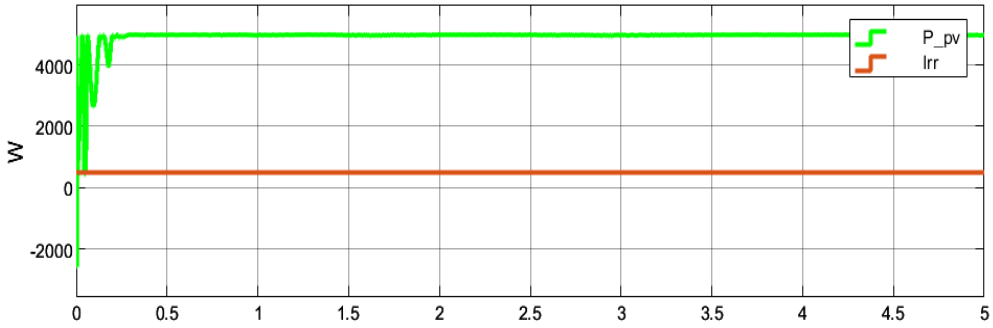

Figure 4.23. MPPT performance in case of 500 W/m2.

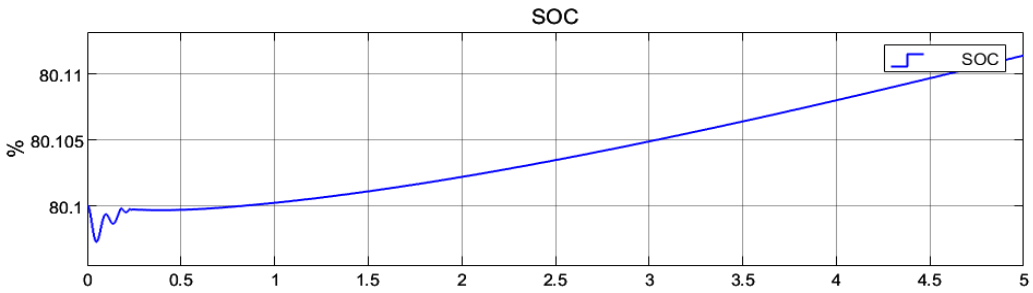

Figure 4.24. Battery SOC curve in case of 500W/m2 and 50% full load.

4.1.6. Case 6: 500 W/m^2 Solar Radiation and Full Load

In this case, radiation level is considered to be 500 W/ m^2. While, full capacity of the system loads is coupled to the system bus. The system voltage and current curves for the case of 500 W/m^2 and full load are presented in figures 4.25 and 4.26 respectively.

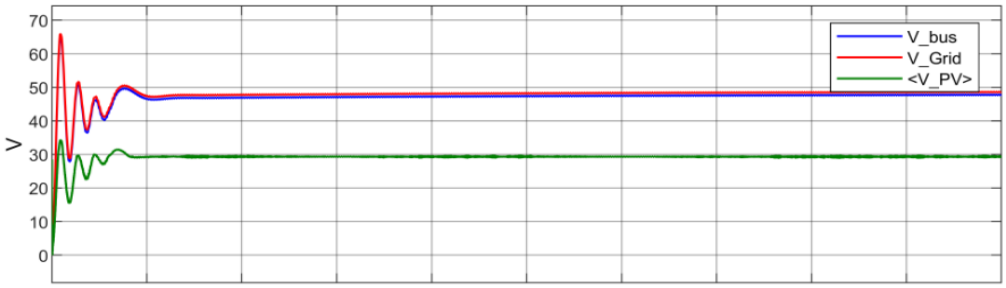

Figure 4.25. System voltage curves in case of 500 W/m2 and full load.

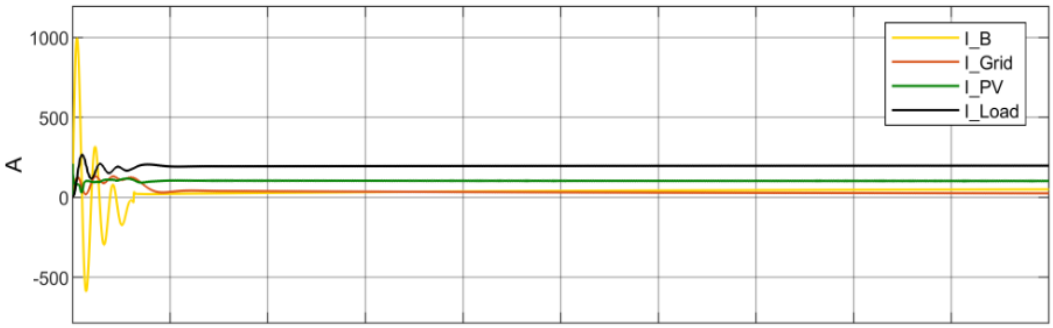

Figure 4.26. System current curves in case of 500 W/m2 and full load.

The MPPT performance is shown in figure 4.27 which contains the PV array power curve and the irradiance level curve.

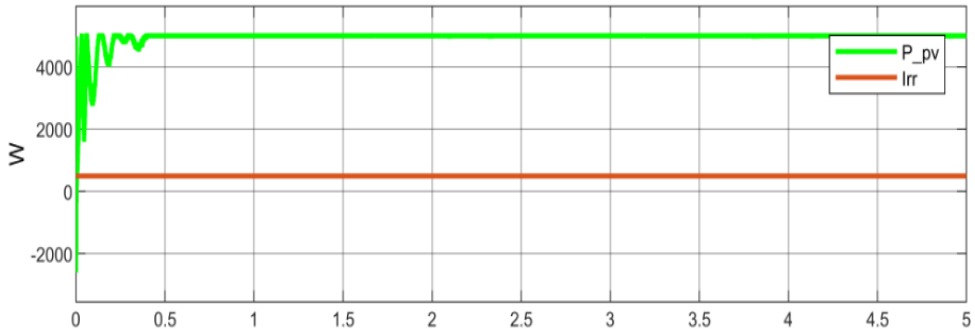

Figure 4.27. MPPT performance in case of 500 W/m2 and full load.

Load sharing is explained in figure 4.28 which shows the system power curves in this case.

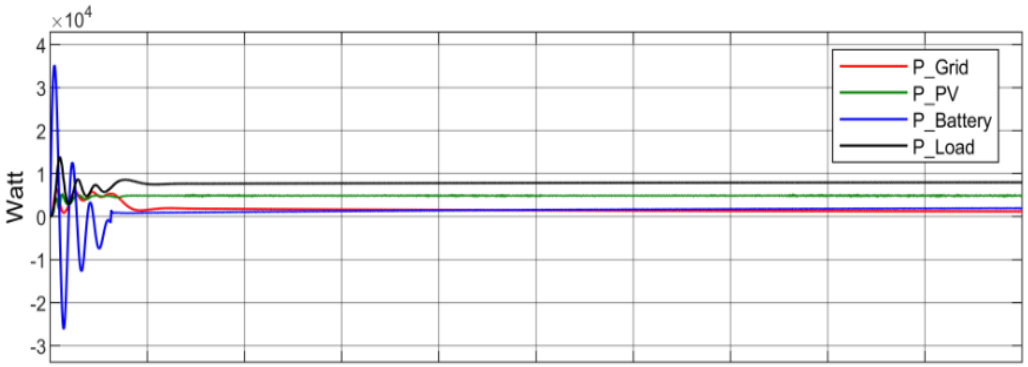

Figure 4.28. System power curves in case of 500 W/m2 and full load.

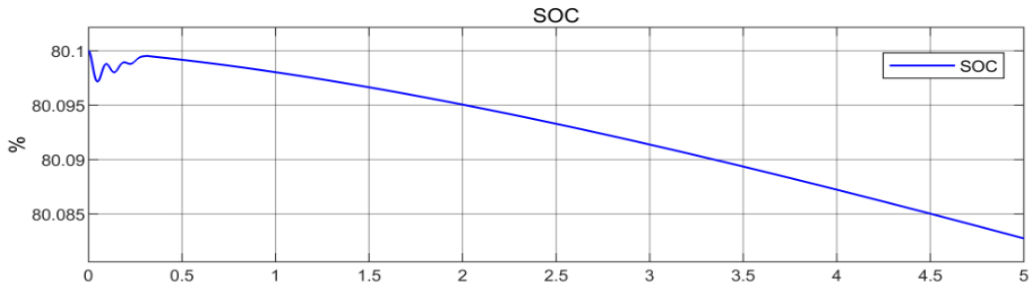

Figure 4.29. Battery SOC curve in case of 500 W/m2 and full load.

Battery charging status is explained in figure 4.29 which shows the battery SOC curve for the case of 500 w/m^2 and full load.

As we see in this case, PV system produces 5 KW real power. And, the total capacity of DC & AC loads connected to the DC bus is 10 KW. So, PV system powers 50% of the loads and battery and national grid powers the rest 50% of the load.

4.1.7. Case 7: 750 W/m^2 Solar Radiation and 25% Full Load

In this case, the PV array works in irradiance level of 750 W/m^2 and 25% of the full loads are connected to the system bus. System voltage curves for this case are presented in figure 4.30, while system currents curves are presented in figure 4.31 and power curve are shown in figure 4.32, MPPT performance is shown in figure 4.33, finally battery state of charge curve is shown in figure 4.34 respectively.

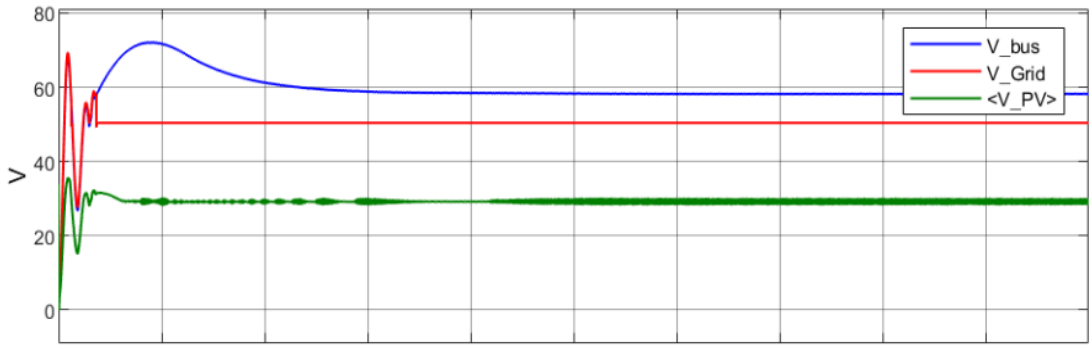

Figure 4.30. System voltage curves in case of 750 W/m2 and 25% full load.

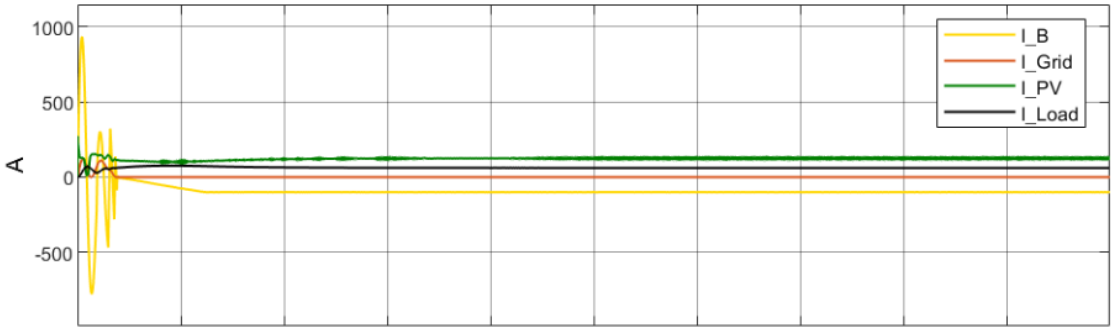

Figure 4.31. System current curves in case of 750 W/m2 and 25% full load.

As we see in this case, PV system produces 7.5 KW real power. And, the total capacity of DC & AC loads connected to the DC bus is 2.5 KW. So, PV system powers 100% of system loads. The battery system does not share in feeding the loads and stays in charging mood and also, national grid does not share in feeding the loads.

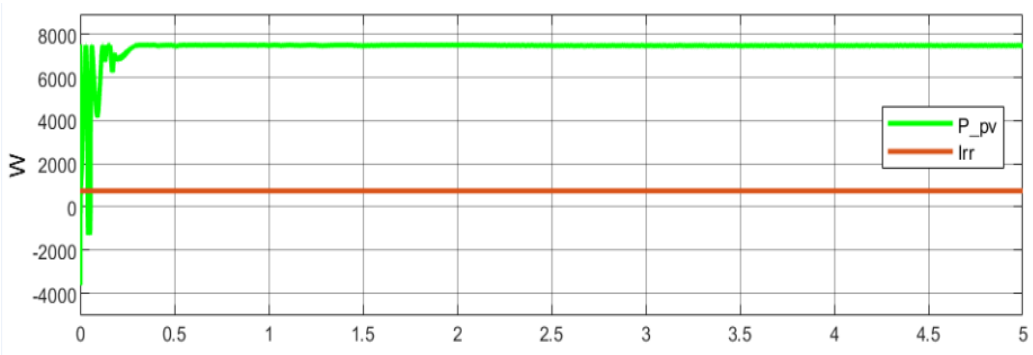

Figure 4.32. MPPT performance in case of 750 w/m2 and 25% full load.

4.1.8. Case 8: 750 W/m^2 Solar Radiation and 50% Full Load

In this case, the PV array works in irradiance level of 750 W/m^2 and 50% of the full loads are connected to the bus. System voltage curves for this case are displayed in figure 4.35, while system currents curves are presented in figure 4.36, System power curves are shown in figure 4.37, MPPT performance is shown in figure 4.38 and finally battery state of charge curve is shown in figure 4.39 respectively.

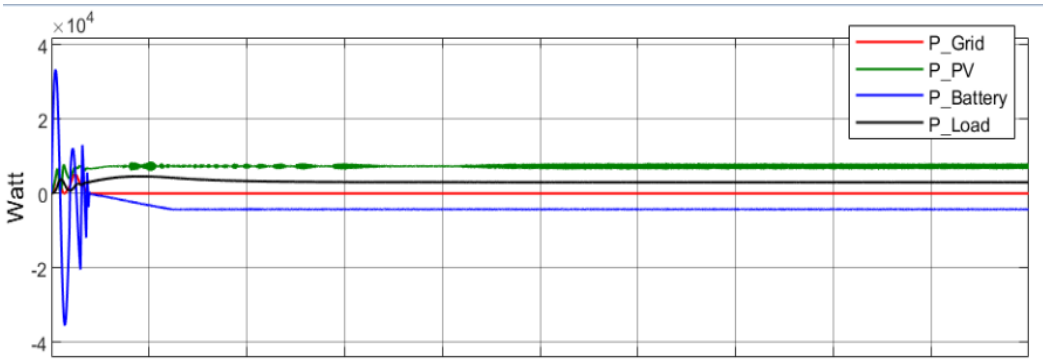

Figure 4.33. System power curves in case of 750 W/m2 and 25% full load

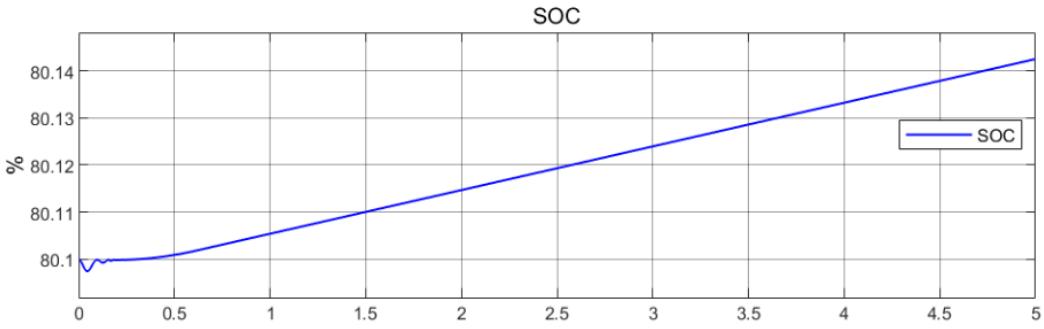

Figure 4.34. Battery SOC curve in case of 750 W/m2 and 25% full load.

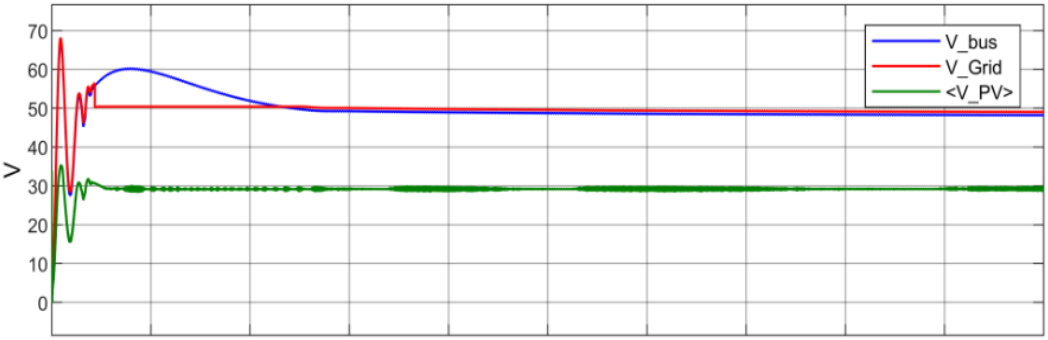

Figure 4.35. System voltage curves in case of 750 W/m2 and 50% full load.

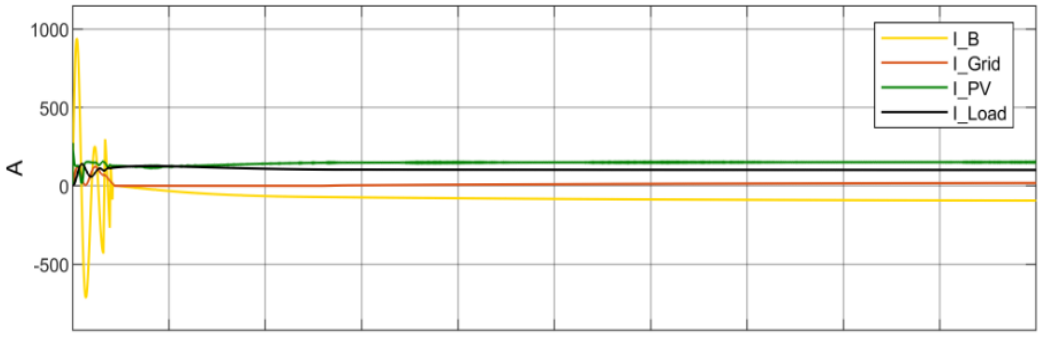

Figure 4.36. System current curves in case of 750 W/m2 and 50% full load.

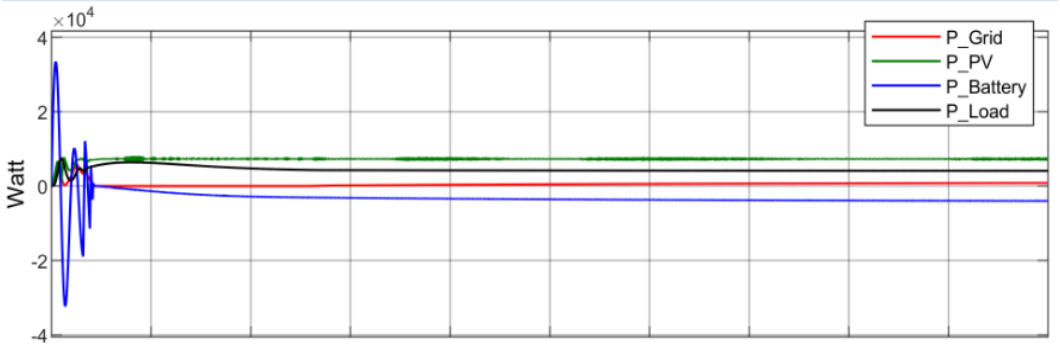

Figure 4.37. System power curves in case of 750 W/m2 and 50% full load.

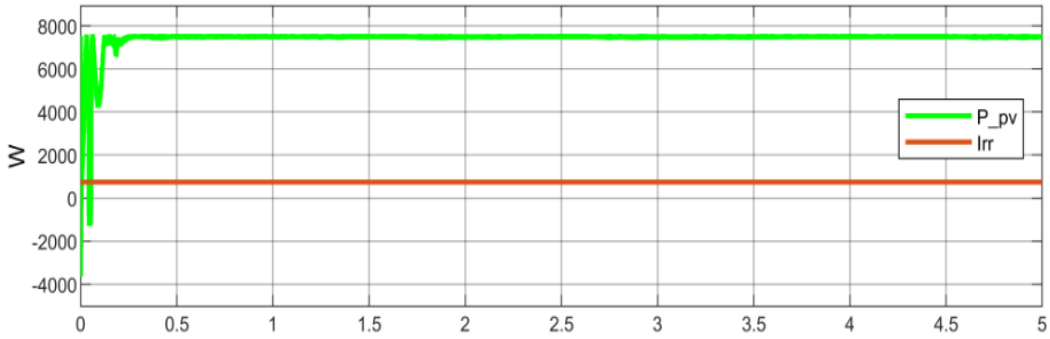

Figure 4.38. MPPT performance in case of 750 W/m2 and 50% full load.

As we see in this case, PV system produces 7.5 KW real power. And, the total capacity of DC & AC loads connected to the DC bus is 5 KW. So, PV system also powers 100% of system loads. The battery system does not share in feeding the loads and stays in charging mood and also, national grid does not share in feeding the loads.

4.1.9. Case 9: 750 W/m^2 Solar Radiation and Full Load

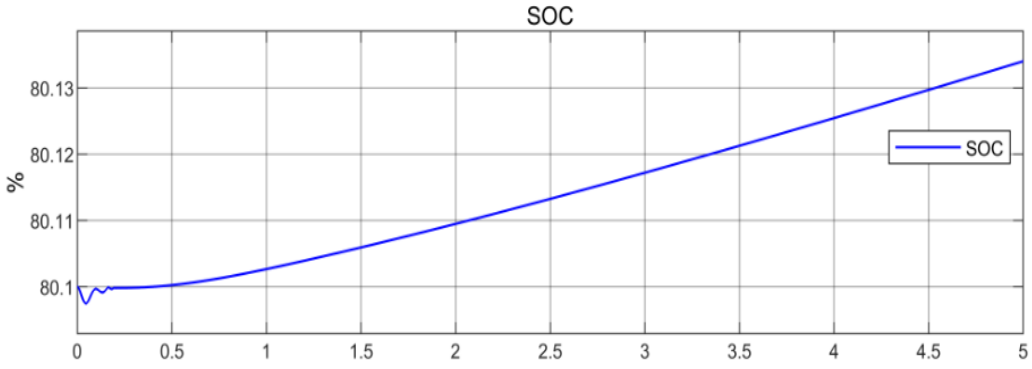

Figure 4.39. Battery SOC curve in case of 750 W/m2 and 50% full load.

In this case, the PV array works in irradiance level of 750 W/m^2 and 100% of the loads are connected to the bus. System voltage curves for this case are shown in figure 4.40, while system currents curves are displayed in figure 4.41, MPPT performance is shown in figure 4.42, system power curves are shown in figure 4.43, and finally battery state of charge curve is shown in figure 4.44 respectively.

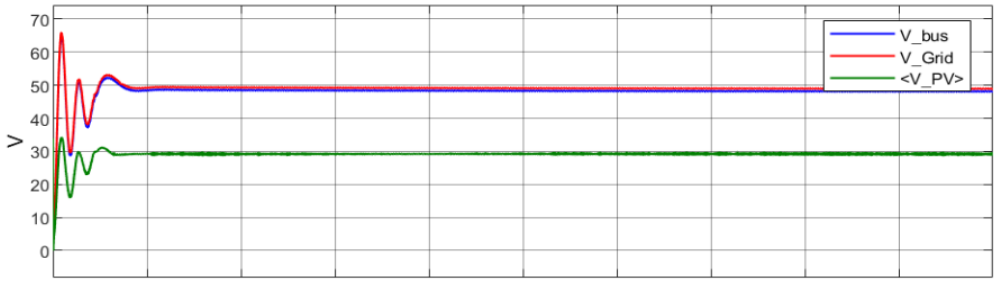

Figure 4.40. System voltage curves in case of 750 W/m2 and full load

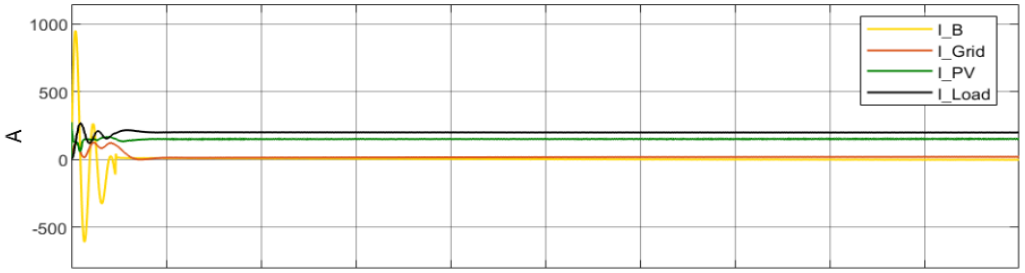

Figure 4.41. System current curves in case of 750 W/m2 and full load.

As we see in this case, PV system produces 7.5 KW real power. And, the total capacity of DC & AC loads connected to the DC bus is 10 KW. So, PV system powers 75% of system loads. The battery system and national grid will power the rest 25 % of system loads.

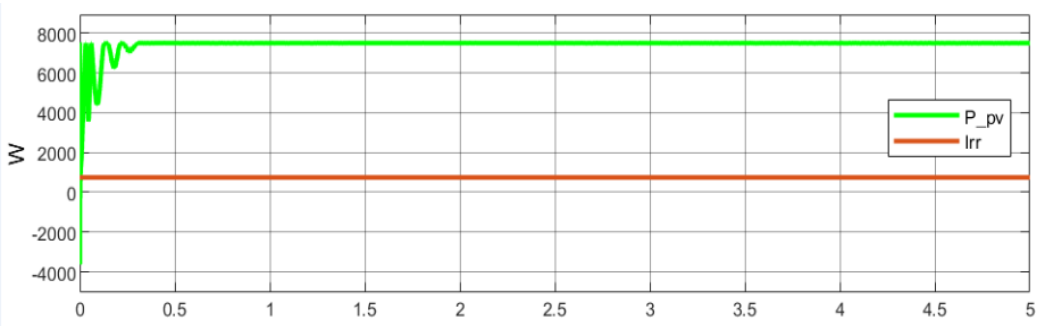

Figure 4.42. MPPT performance in case of 750 W/m2 and full load.

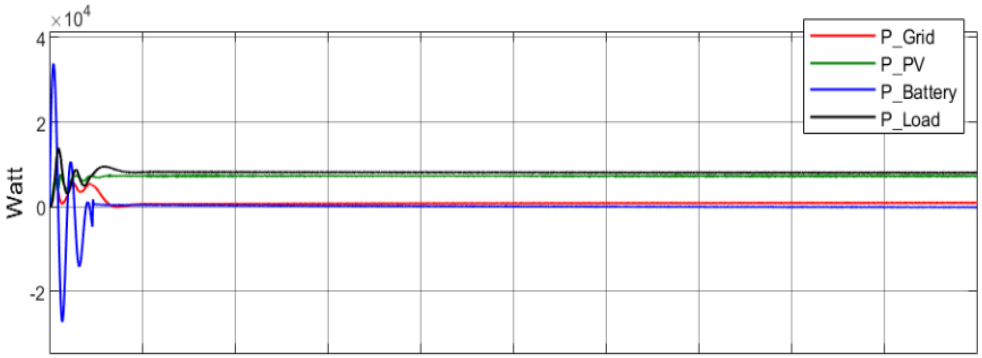

Figure 4.43. System power curves in case of 750 W/m2 and full load.

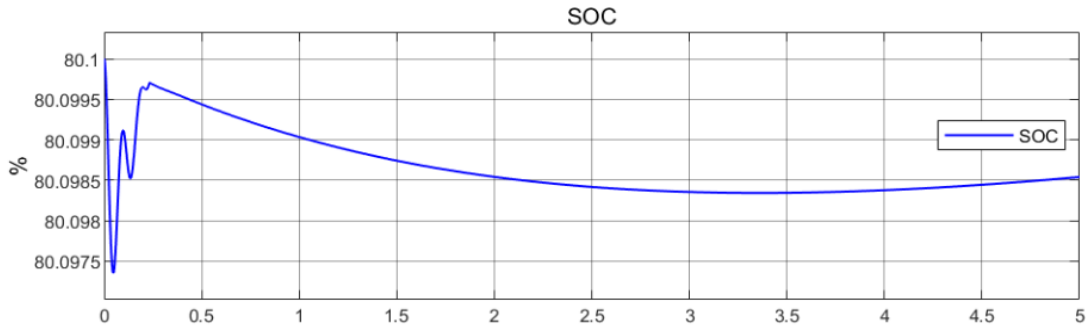

Figure 4.44. Battery state of charge curve.

4.1.10. Case 10: 1000 W/m^2 Solar Radiation and 25% Full Load

In this case, full irradiance level 1000 W/m^2 is considered. The real power produced by the PV array is 10 KW. While, the system is loaded with 25% of the full load. System voltage curves for this case are shown in figure 4.45, while figure 4.46 displays the system current curves for the same curves.

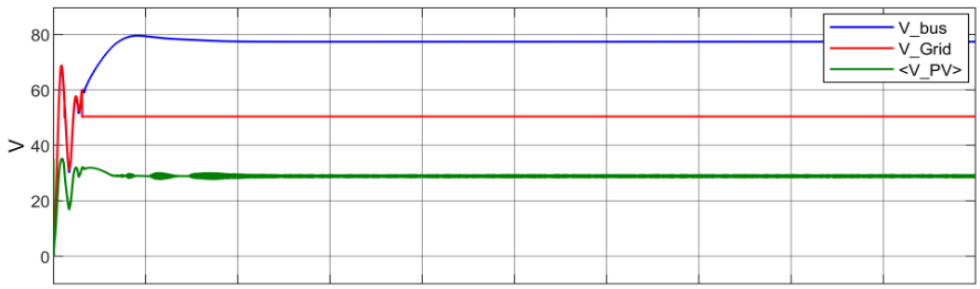

Figure 4.45. System voltage curves in case of 1000 W/m2 and 25% full load.

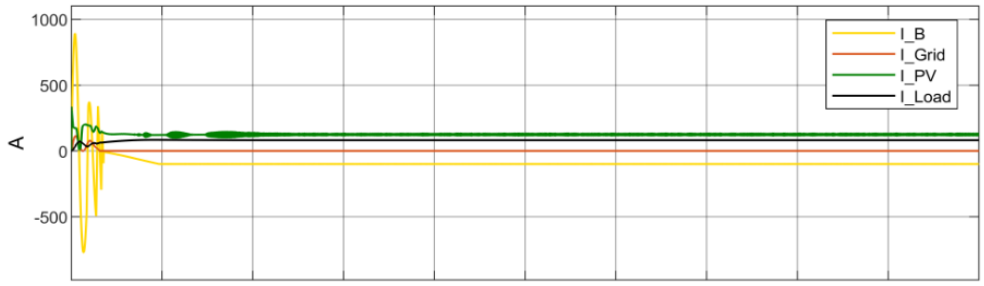

Figure 4.46. System current curves in case of 1000 W/m2 and 25% full load.

The MPPT performance is shown in figure 4.47 which contains the PV power curve and irradiance level curve.

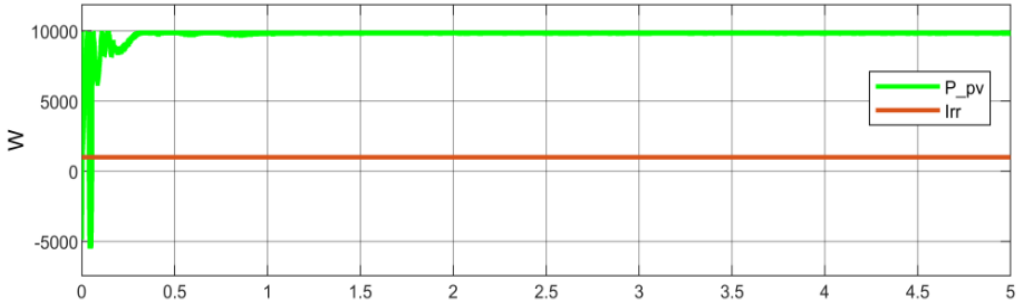

Figure 4.47. MPPT performance in case of 1000 W/m2 and 25% full load.

System power curves are shown in figure 4.48, as we see in this case, that the PV array system produces 10 KW. While, the system is loaded only by 2.5 KW. So, the produced power higher than the load demand, and therefore the battery goes through charging mode as presented in figure 4.49 which shows the SOC of the battery.

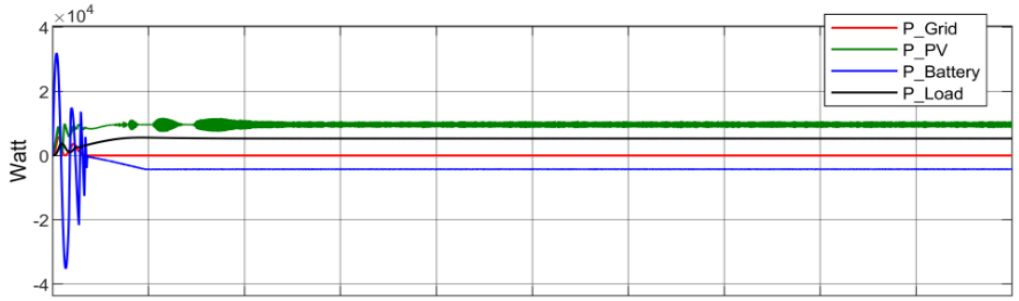

Figure 4.48. System power curves in case of 1000 W/m2 and 25% full load.

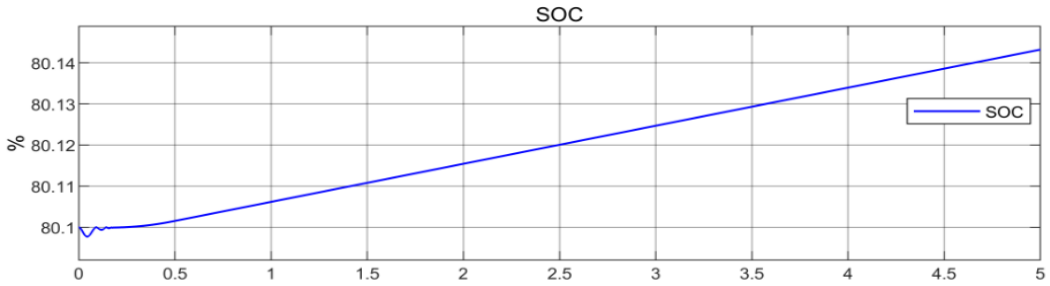

Figure 4.49. Battery SOC in case of 1000 W/m2 and 25% full load.

4.1.11. Case 11: 1000 W/m^2 Solar Radiation and 50% full Load

In this case, the loads connected to the bus system is increased to be 50% of the full load. While, the irradiance level is assumed to be 1000 W/m^2. The system voltage curves are shown in figure 4.50 and system current curves are shown in figure 4.51.

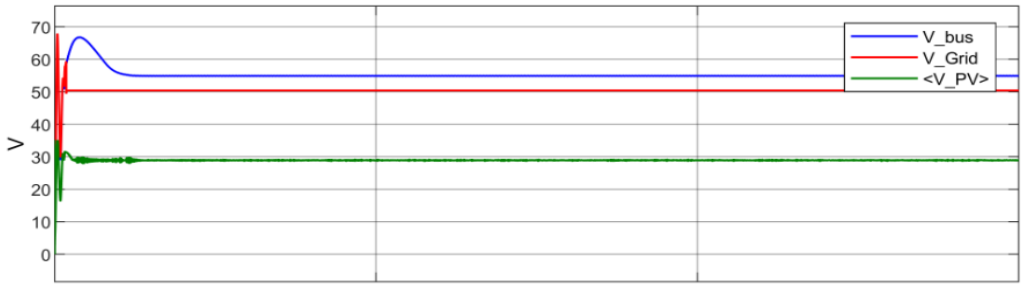

Figure 4.50. System voltage curves in case of 1000 W/m2 and 50% full load.

The PV power curve and irradiance level curve are shown in figure 4.52, which shows the high performance of the MPPT operation. System load sharing is explained in figure 4.53 which contains the power curves of the system.

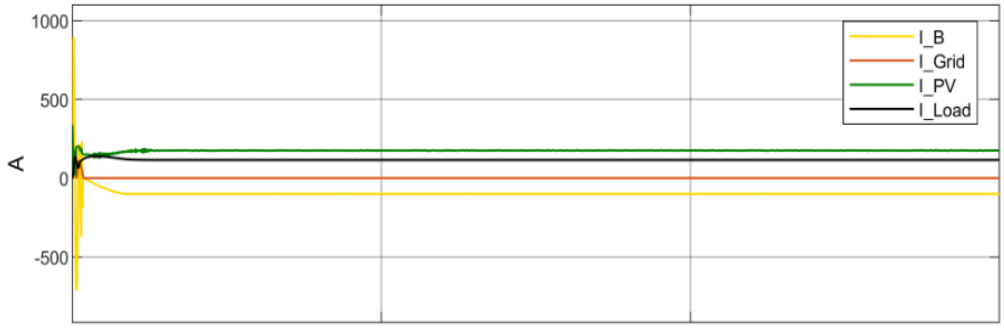

Figure 4.51. System current curves in case of 1000 W/m2 and 50% full load.

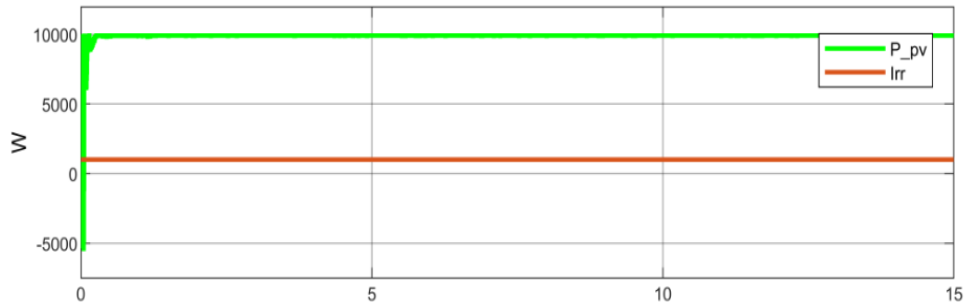

Figure 4.52. MPPT performance in case of 1000 W/m2 and 50% full load.

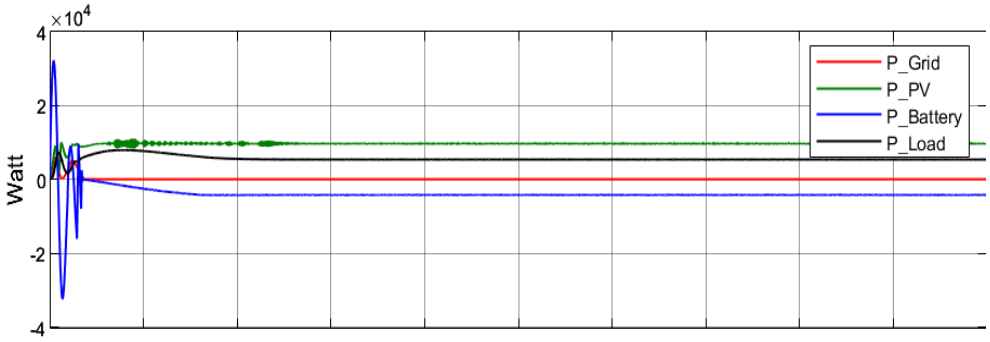

Figure 4.53. System power curves in case of 1000 W/m2 and 50% full load.

It is clear in this case, that the PV array system produces 10 KW. While, the system is loaded only by 5 KW. So, the produced power is still greater than the load demand, and therefore the battery system stays in charging mode. While, the national grid does not share in feeding the load.

4.1.12. Case 12: 1000 W/m^2 Solar Radiation and Full Load

In this case, the irradiance level is assumed to be 1000 w/m^2 and the system is loaded with its full load. The power produced by PV array is 10 KW. Figures 4.54 and 4.55 show the system voltage and current curves in this case.

Figure 4.54. System voltage curves in case of 1000 W/m2 and full load.

The MPPT performance is shown in figure 4.56, which shows the high performance for MPPT and not affected by the load change.

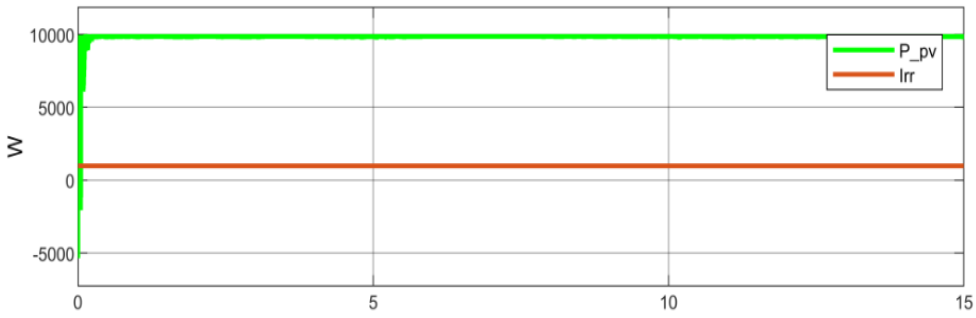

Figure 4.55. MPPT performance in case of 1000 W/m2 and full load.

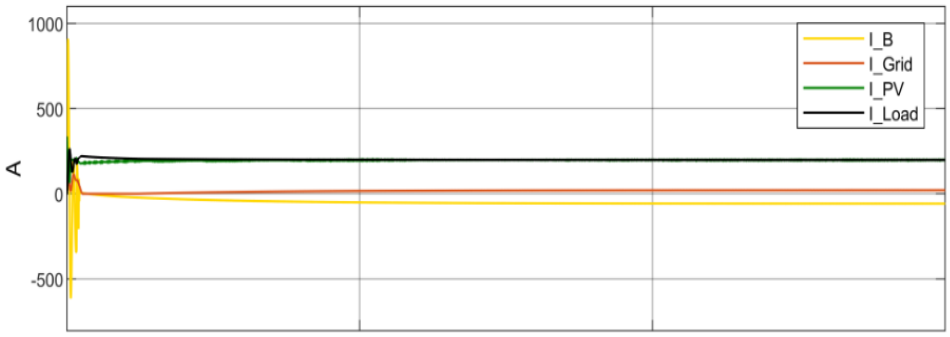

Figure 4.56. System current curves in case of 1000 W/m2 and full load.

The load sharing process is shown in figure 4.57, which displays the system power curves. While, the battery SOC is shown in figure 4.58.

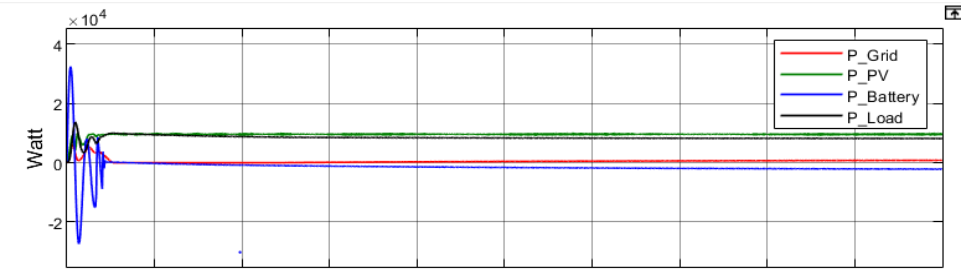

Figure 4.57. System power curves in case of 1000 W/m2 and full load.

It is clear in this case, that the PV array system produces 10 KW. And also, the system is loaded by 10 KW. So, the PV system powers 100 % of loads. While, battery system and national grid do not share in feeding the loads.

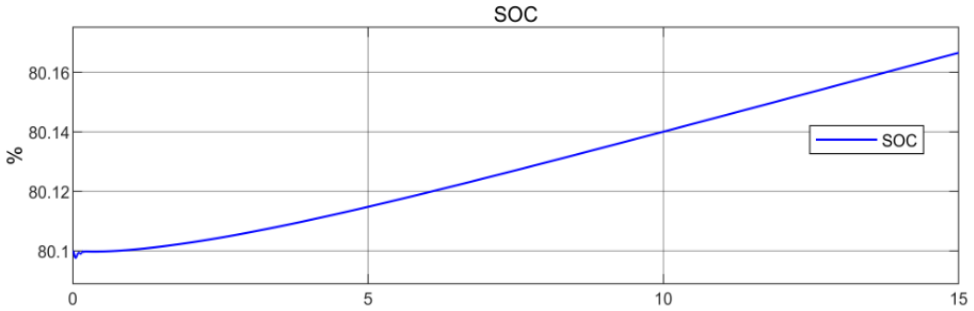

Figure 4.58. Battery SOC in case of 1000 W/m2 and full load.

4.1.13. Case 13: PV Array Idle and System Is Full Loaded

In this case all the load is supplied from the grid and the battery system. The system voltage curves are shown in figure 4.59, it is clear that the PV array voltage is 0V in this case.

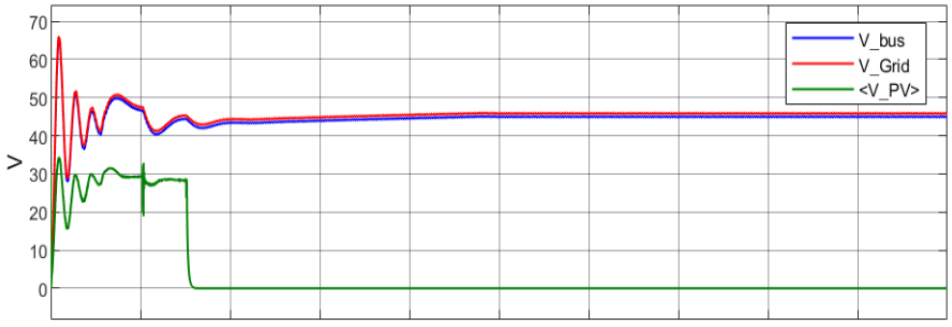

Figure 4.59. System voltage curves in case of idle PV and full load

The system current curves are shown in figure 4.60, also it is clear that the load current equal to the sum of battery current and grid current and that means the load is shared between them.

System power curves show that the PV array did not produce any real power while the load is supplied from the grid and the battery as presented in figure 4.61. Battery response is displayed in figure 4.62.

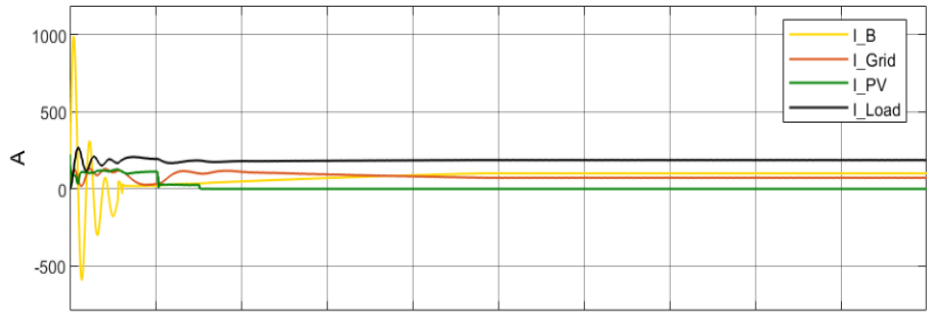

Figure 4.60. System current curves in case of idle PV and full load.

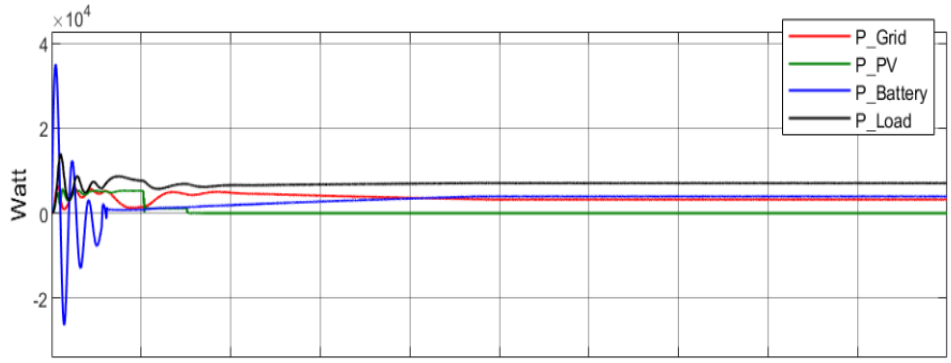

Figure 4.61. System power curves in case of idle PV array and full load.

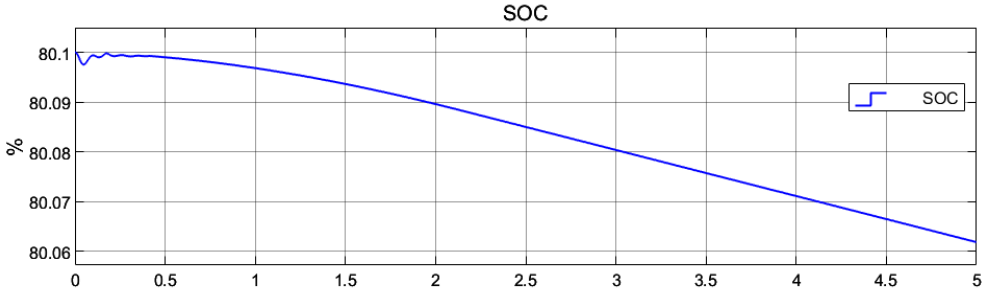

Figure 4.62. Battery SOC in case of idle PV array and full load.

PART 5

CONCLUSSIONS AND RECOMMONDATIONS

This chapter presents the most important conclusions that have been reached by studying the exploitation of the grid connected DC microgrid with renewable energy source and battery bank system. It also presents the recommendations and future works that depend on the proposed system simulation results.

5.1. CONCLUSSIONS

The studied grid connected DC microgrid that consists of DC load, AC load, PV array with MPPT system and battery storage system as explained in figure 3.1 is simulated for all expected operating cases. The irradiance level graduated from zero W/m2 until 1000 W/m2. Thirteen operating cases are simulated. In all cases, the PV array system worked in maximum power. The use of P&O MPPT algorithm gives the proposed DC-DC boost converter the ability to track the maximum power point with high performance.

The load sharing between the utility grid and the PV array with battery bank system is clear in studied cases, while the priority selected to supply the loads from the PV panel and battery bank system and when these two sources are less than the load demand, the utility grid will complete the required energy amount. The BMS designed in such way that makes the battery goes through charging process depending on the PV array system power only and also makes the battery goes to the process of supplying the loads when the power produced by the PV array is lower than the load demand, also prevent battery charging from the utility grid.

The simulation results confirm the good performance of proposed system, in both high and low irradiance level, therefore the proposed system can be used in clear and

cloudy weather. The minimum capacity of the storage battery system must be higher than the difference between the PV array maximum power and the load capacity to ensure storing all the PV energy that exceeds the load demand.
The isolation of controllers (MMPT & BMS) makes the system more reliable and gives it fast response.

5.2. FUTURE WORKS

Depending on the studied system simulation results, there is a list of works or modifications that can be suggested to be a future works for the other researchers.

1. Use push-pull DC/DC converter for MPPT instead of boost converter since this type of converters can be used with high rated power than the boost converters.
2. Use controlled rectifiers in AC utility grid with power factor correction algorithms to connect the AC grid with the DC micro grid to keep the power quality as high as possible in the utility grid.

REFERENCES

[1] A. Ipakchi and F. Albuyeh, “Grid of the future,” *IEEE power energy Mag.*, vol. 7, no. 2, pp. 52–62, 2009.

[2] H. Farhangi, “The path of the smart grid,” IEEE Power Energy Mag., vol. 8, no. 1, pp. 18–28, January 2010.

[3] H. Li et al., “Lifetime test design for second-use electric vehicle batteries in residential applications,” IEEE Trans. Sustain. Energy, vol. 8, no. 4, pp. 1736–1746, Oct 2017.

[4] Li, He, et al. "Usage profile optimization of the retired PHEV battery in residential microgrid." *2014 IEEE Conference and Expo Transportation Electrification Asia-Pacific (ITEC Asia-Pacific)*. IEEE, 2014.

[5] H. Li, F. Guo, S. Yang, L. Zhu, C. Yao, and J. Wang, “Usage profile optimization of the retired PHEV battery in residential microgrid,” in *2014 IEEE Conference and Expo Transportation Electrification Asia-Pacific (ITEC Asia-Pacific)*, 2014, pp. 1–6.

[6] Basso, Tim. "IEEE standard for interconnecting distributed resources with the electric power system." *IEEE Pes Meeting*. 2004..

[7] Katiraei, Farid, et al. "Microgrids management." *IEEE power and energy magazine* 6.3 (2008): 54-65..

[8] R. Lasseter, J. Eto, B. Schenkman, J. Stevens, H. Vollkommer, D. Klapp, E. Linton, H. Hurtado, and J. Roy, “Certs microgrid laboratory test bed,” IEEE Trans. Power Del., vol. 26, no. 1, pp. 325–332, Jan 2011.

[9] H. Nikkhajoei and R. Lasseter, “Distributed generation interface to the certs microgrid,” IEEE Trans. Power Del., vol. 24, no. 3, pp. 1598–1608, July 2009.

[10] T. Dragičević, X. Lu, J. C. Vasquez, and J. M. Guerrero, “DC microgrids—Part II: A review of power architectures, applications, and standardization issues,” *IEEE Trans. power Electron.*, vol. 31, no. 5, pp. 3528–3549, 2015.

[11] S. Anand, B. G. Fernandes, and J. Guerrero, “Distributed control to ensure proportional load sharing and improve voltage regulation in low-voltage DC microgrids,” *IEEE Trans. power Electron.*, vol. 28, no. 4, pp. 1900–1913, 2012.

[12] S.-I. Go and J.-H. Choi, “Design and dynamic modelling of pv-battery hybrid systems for custom electromagnetic transient simulation,” *Electronics*, vol. 9, no. 10, p. 1651, 2020.

[13] Gao, David Wenzhong. *Energy storage for sustainable microgrid*. Academic Press, 2015.

[14] K. Shah, P. Chen, A. Schwab, K. Shenai, S. Gouin-Davis, and L. Downey, "Smart efficient solar DC micro-grid," in *2012 IEEE Energytech*, 2012, pp. 1–5.

[15] B. Kroposki, C. Pink, R. DeBlasio, H. Thomas, M. Simoes, and P. K. Sen, "Benefits of power electronic interfaces for distributed energy systems," *IEEE Trans. energy Convers.*, vol. 25, no. 3, pp. 901–908, 2010.

[16] M. F. Akorede, H. Hizam, and E. Pouresmaeil, "Distributed energy resources and benefits to the environment," *Renew. Sustain. energy Rev.*, vol. 14, no. 2, pp. 724–734, 2010.

[17] T. Adefarati, N. B. Papy, M. Thopil, and H. Tazvinga, "Non-renewable distributed generation technologies: A review," *Handb. Distrib. Gener.*, pp. 69–105, 2017.

[18] J. Choi, *Survivability on Prime Mover-powered Distributed Energy Resources Under Transient Overload Conditions During Microgrid Islanding*. The Ohio State University, 2019.

[19] S. Bahramirad, W. Reder, and A. Khodaei, "Reliability-constrained optimal sizing of energy storage system in a microgrid," *IEEE Trans. Smart Grid*, vol. 3, no. 4, pp. 2056–2062, 2012.

[20] J. M. Guerrero, J. C. Vasquez, J. Matas, L. G. De Vicuña, and M. Castilla, "Hierarchical control of droop-controlled AC and DC microgrids—A general approach toward standardization," *IEEE Trans. Ind. Electron.*, vol. 58, no. 1, pp. 158–172, 2010.

[21] M. Mokhtar, M. I. Marei, and A. A. El-Sattar, "A control scheme for islanded and grid-connected DC microgrids," in *2017 Nineteenth International Middle East Power Systems Conference (MEPCON)*, 2017, pp. 176–180.

[22] R. A. F. Ferreira, H. A. C. Braga, A. A. Ferreira, and P. G. Barbosa, "Analysis of voltage droop control method for dc microgrids with Simulink: Modelling and simulation," in *2012 10th IEEE/IAS International Conference on Industry Applications*, 2012, pp. 1–6.

[23] G. Niyitegeka, J. Choi, and Y. Ok, "Improved droop control for effective load sharing and voltage regulation in DC microgrids," in *2016 Electric Power Quality and Supply Reliability (PQ)*, 2016, pp. 125–132.

[24] D. W. Gao, *Energy storage for sustainable microgrid*. Academic Press, 2015.

[25] A. A. Servansing, *A Parallel-Series Two Bridge DC/DC Converter for PV Power Conditioning Systems Used in Hybrid Renewable Energy Systems*. Queen's University (Canada), 2012.

[26] Y. Zhang and Y. W. Li, “Energy management strategy for supercapacitor in droop-controlled DC microgrid using virtual impedance,” *IEEE Trans. Power Electron.*, vol. 32, no. 4, pp. 2704–2716, 2016.

[27] A. Varghese, L. R. Chandran, and A. Rajendran, “Power flow control of solar PV based islanded low voltage DC microgrid with battery management system,” in *2016 IEEE 1st International Conference on Power Electronics, Intelligent Control and Energy Systems (ICPEICES)*, 2016, pp. 1–6.

[28] D. H. Tungadio and Y. Sun, “Active power management of islanded interconnected distributed generation,” *Int. J. Electr. Electron. Eng. Telecommun.*, vol. 9, pp. 177–182, 2020.

[29] K. E. Muehlegg, “Modelling and Energy Management for DC Microgrid Systems.” University of Toronto (Canada), 2017.

[30] J. Sun, W. Lin, M. Hong, and K. A. Loparo, “Voltage regulation of DC-microgrid with PV and battery: A passivity method,” *IFAC-PapersOnLine*, vol. 52, no. 16, pp. 753–758, 2019.

[31] Y. Li, W. Gao, and Y. Ruan, “Performance investigation of grid-connected residential PV-battery system focusing on enhancing self-consumption and peak shaving in Kyushu, Japan,” *Renew. energy*, vol. 127, pp. 514–523, 2018.

[32] V. Nikam and V. Kalkhambkar, “A review on control strategies for microgrids with distributed energy resources, energy storage systems, and electric vehicles,” *Int. Trans. Electr. Energy Syst.*, vol. 31, no. 1, p. e12607, 2021.

[33] J. A. Grant, “Design and Simulation of a DC Microgrid for a Small Island in Belize,” *Sustain. Energy Eng. Sch. Energy*, 2018.

[34] S. Zhang and Y. Tang, “Optimal schedule of grid-connected residential PV generation systems with battery storages under time-of-use and step tariffs,” *J. Energy Storage*, vol. 23, pp. 175–182, 2019.

[35] S. U. Rehman, S. Rehman, M. Shoaib, and I. A. Siddiqui, “Feasibility study of a grid-tied photovoltaic system for household in Pakistan: considering an unreliable electric grid,” *Environ. Prog. Sustain. Energy*, vol. 38, no. 3, p. e13031, 2019.

[36] I. Javeed, R. Khezri, A. Mahmoudi, A. Yazdani, and G. M. Shafiullah, “Optimal sizing of rooftop PV and battery storage for grid-connected houses considering flat and time-of-use electricity rates,” *Energies*, vol. 14, no. 12, p. 3520, 2021.

[37] S. B. Sepúlveda-Mora and S. Hegedus, “Making the case for time-of-use electric rates to boost the value of battery storage in commercial buildings with grid connected PV systems,” *Energy*, vol. 218, p. 119447, 2021.

[38] J. Mannan, M. A. Kamran, M. U. Ali, and M. M. N. Mannan, “Quintessential strategy to operate photovoltaic system coupled with dual battery storage and grid connection,” *Int. J. Energy Res.*, vol. 45, no. 15, pp. 21140–21157, 2021.

[39] M. C. Argyrou, C. C. Marouchos, S. A. Kalogirou, and P. Christodoulides, "Modeling a residential grid-connected PV system with battery–supercapacitor storage: Control design and stability analysis," *Energy Reports*, vol. 7, pp. 4988–5002, 2021.

[40] J. Sun, D. M. Mitchell, M. F. Greuel, P. T. Krein, and R. M. Bass, "Averaged modeling of PWM converters operating in discontinuous conduction mode," *IEEE Trans. power Electron.*, vol. 16, no. 4, pp. 482–492, 2001.

[41] S. D. Sudhoff, "Buck Converter Design," *Power Magn. Devices*, no. January, pp. 461–502, 2021, doi: 10.1002/9781119674658.ch13.

[42] Y. Huang, F. Z. Peng, J. Wang, and D. Yoos, "Survey of the power conditioning system for PV power generation," in *2006 37th IEEE Power Electronics Specialists Conference*, 2006, pp. 1–6.

[43] T. Esram and P. L. Chapman, "Comparison of photovoltaic array maximum power point tracking techniques," *IEEE Trans. energy Convers.*, vol. 22, no. 2, pp. 439–449, 2007.

[44] S. Sholapur, K. R. Mohan, and T. R. Narsimhegowda, "Boost converter topology for pv system with perturb and observe mppt algorithm," *IOSR J. Electr. Electron. Eng.*, vol. 9, no. 4, pp. 50–56, 2014.

[45] B. Bendib, H. Belmili, and F. Krim, "A survey of the most used MPPT methods: Conventional and advanced algorithms applied for photovoltaic systems," *Renew. Sustain. Energy Rev.*, vol. 45, pp. 637–648, 2015.

[46] A. Moghassemi, S. Ebrahimi, and J. Olamaei, "Maximum power point tracking methods used in photovoltaic systems: A review," *Signal Process. Renew. energy*, vol. 4, no. 3, pp. 19–39, 2020.

[47] Karami, Nabil, Nazih Moubayed, and Rachid Outbib. "General review and classification of different MPPT Techniques." *Renewable and Sustainable Energy Reviews* 68 (2017): 1-18.

[48] Faranda, Roberto, and Sonia Leva. "Energy comparison of MPPT techniques for PV Systems." *WSEAS transactions on power systems* 3.6 (2008): 446-455.

[49] Nedumgatt, Jacob James, et al. "Perturb and observe MPPT algorithm for solar PV systems-modeling and simulation." *2011 Annual IEEE India Conference*. IEEE, 2011.

[50] M. H. Rashid, *Power electronics: circuits, devices, and applications*. Pearson Education India, 2009.

[51] D. M. Mitchell, *DC-DC switching regulator analysis*. McGraw-Hill Companies, 1988.

[52] H. Cai, J. Xiang, W. Wei, and M. Z. Q. Chen, "$ V $–${d} p/{d} v $ Droop Control for PV Sources in DC Microgrids," *IEEE Trans. Power Electron.*, vol.

33, no. 9, pp. 7708–7720, 2017.

[53] Lee, Hoon, et al. "Energy Management System of DC Microgrid in Grid-Connected and Stand-Alone Modes: Control, Operation and Experimental Validation." *Energies* 14.3 (2021): 581.

[54] A. Kamel, Ahmed, et al. "Energy management of a DC microgrid composed of photovoltaic/fuel cell/battery/supercapacitor systems." *Batteries* 5.3 (2019): 63.

[55] S. Sumathi, L. A. Kumar, and P. Surekha, Solar PV and Wind Energy Conversion Systems: An Introduction to Theory, Modeling with MATLAB/SIMULINK, and the Role of Soft Computing Techniques. Springer, 2015.

[56] Karshenas, Hamid R., et al. "Bidirectional dc-dc converters for energy storage systems." *Energy storage in the emerging era of smart grids* 18 (2011).

[57] H. Cha and S. Lee, "Design and implementation of photovoltaic power conditioning system using a current based maximum power point tracking," in *2008 IEEE Industry Applications Society Annual Meeting*, 2008, pp. 1–5.

[58] N. Javaid *et al.*, "An intelligent load management system with renewable energy integration for smart homes," *IEEE access*, vol. 5, pp. 13587–13600, 2017.

RESUME

Waleed Khalid Abdulkareem AL-BAYATI, working as Admin & OPS officer with Heartland Alliance International organization. He got his bachelor degree in Electrical Engineering from Kirkuk University and He is completing his master degree in Electrical Engineering in Karabuk University in Turkey.